UNIVERSITÀ
DEGLI STUDI
FIRENZE

DOTTORATO DI RICERCA IN
SCIENZE DELLA TERRA

CICLO XXVII

COORDINATORE Prof. LORENZO ROOK

Interaction Processes Between Biota and Natural Inorganic Systems: Environmental Applications

Settore Scientifico Disciplinare GEO/06

Dottorando

Dott. Tiziano Catelani

Tutore

Prof. Giovanni Pratesi

Co-Tutore

Prof. Pilario Costagliola

Coordinatore

Prof. Lorenzo Rook

Anni 2012/2016

“Then the moment will come,

and the memory will shine”

INDEX

Abstract

Bio-mediated and chemical processes for Arsenic uptake in calcite were investigated by means of synchrotron radiation techniques (XAS, CTR, RAXR) coupled with more traditional mineralogical analysis (XRD, XRF). The processes are presented here in two distinct works. Regarding the Arsenic uptake in bacterial calcite, our study began with the characterization of Bullicame Hot Springs (Viterbo, Italy) where naturally As-enriched travertines precipitate. From such hot springs bacteria were sampled and cultured in laboratory, selecting the strains which were more resistant to high As concentrations and were able to precipitate calcite. Among the 65 strains isolated, *B.licheniformis* was selected for bio-mediated calcite precipitation experiments both in liquid and solid medium. Bacterial calcites were characterized by means of XRD, XRF and XAS in order to investigate As trapping. The main outcomes regards the positive effect of Mg in incorporating As in calcite, the effect of As on calcite structure, and the role of bacteria and their living environment in regulating the As cycle. In particular we demonstrate that bacterial precipitation process allow Arsenite uptake in calcite differently form the chemical process. Medium properties and the presence of Magnesium have been observed to be critical parameters of this process.

Regarding the chemical process we focused both on Arsenic and Mercury, two environmentally dangerous elements. Uptake experiments on calcite-(104) surface were performed by means of *in situ* experiments with liquid cell AFM and X-Ray Reflectivity techniques (CTR and RAXR), in order to investigate in depth the adsorption and incorporation during calcite-(104) epitaxial growth. Regarding Arsenic we observed that uptake process results efficient only for Arsenate which partially influences calcite surface structure, while Arsenite uptake is almost negligible. More in detail, our results suggest that Arsenate uptake passes through surface adsorption and subsequent ordering in calcite crystal lattice substituting carbonate during crystal growth. Regarding Mercury, we observed the effective uptake in calcite but our results do not clearly resolve if Hg^{2+} substitutes Ca^{2+} in calcite crystal structure. On the other hand we found that Mercury trapped in calcite seems to be unstable causing surface relaxation with mineral aging with re-ordering of surface structure.

Riassunto

Nel presente lavoro di tesi sono stati studiati i processi di incorporazione dell'Arsenico in calcite per via chimica e per via bio-mediata mediante tecniche che fanno uso di radiazione di sincrotrone (XAS, CTR, RAXR) associati a tecniche più tradizionali di analisi mineralogica (XRD, XRF). I due processi sono qui presentati in due lavori distinti. Per quanto riguarda l'assorbimento di arsenico in calcite batterica, il nostro studio è iniziato con la caratterizzazione delle sorgenti termali del Bullicame (Viterbo, Italia) dove sono stati riscontrati elevati tenori di arsenico nelle acque profonde e sorgive, e nei travertini che precipitano in prossimità delle sorgenti. Da queste sorgenti termali sono state campionate acque e travertini di neo formazione, dai quali sono stati coltivati e isolati in laboratorio dei ceppi batterici. Successivamente fra i 65 ceppi batterici isolati sono stati selezionati quelli che erano più resistenti alle alte concentrazioni di Arsenico e che erano in grado di precipitare rapidamente calcite. Infine solo *B. licheniformis* è stato selezionato per esperimenti di precipitazione di calcite bio-mediata in terreno liquido e solido. Le calciti batteriche sono state caratterizzate mediante XRD, XRF e XAS al fine di indagare in che modo avviene il processo di intrappolamento dell'Arsenico. I principali risultati riguardano l'effetto del Magnesio sulla capacità di incorporare Arsenico in calcite, l'effetto dell'Arsenico sulla struttura calcite, e il ruolo dei batteri e dell'ambiente in cui essi vivono nella regolazione del ciclo dell'Arsenico. In particolare abbiamo dimostrato che il processo di precipitazione di calcite batterica consente la precipitazione dello ione Arsenito nella calcite differentemente da quanto avvenga nel processo chimico. Per quanto riguarda il processo chimico ci siamo concentrati, oltre che sullo studio dell'Arsenico, pure su quello del Mercurio, entrambi elementi pericolosi per l'uomo. Nello specifico sono stati condotti esperimenti *in situ* di crescita epitassiale sulla superficie cristallografica (104) con AFM in cella liquida e successivamente con tecniche di riflessione speculare dei Raggi X in luce di sincrotrone (CTR e RAXR) con lo scopo di indagare in modo approfondito l'adsorbimento e l'incorporazione durante la precipitazione di calcite da soluzioni arricchite in Arsenico e Mercurio. Per quanto riguarda l'Arsenico abbiamo osservato che il processo di intrappolamento è efficacie solo per la forma ossidata (ione Arsenato) che influenza in modo evidente la struttura superficiale della calcite, mentre l'incorporazione della forma ridotta (Arsenito) è quasi del tutto trascurabile. Più in dettaglio, i nostri risultati suggeriscono che l'incorporazione dell'Arsenato passa attraverso un processo di adsorbimento superficiale e successivo ordinamento nel reticolo cristallino della calcite, sostituendo carbonato. Per quanto riguarda il Mercurio, abbiamo osservato l'incorporazione in calcite risulta efficace, ma i nostri risultati non risolvono in modo univoco se Hg^{2+} sostituisca o meno Ca^{2+} nella

struttura della calcite. D'altra parte, abbiamo invece riscontrato che il Mercurio intrappolato in calcite sembra essere instabile producendo un rilassamento della superficie della calcite e probabilmente essoluzione di fasi arricchite in Mercurio.

INTRODUCTION

The interactions between biosphere and geosphere is a subject nowadays still poorly understood. In fact, despite it is well known that the living beings appearance on Earth has radically changed our planet evolution, the interactions between biota and the abiotic world have been neglect for long. Actually, it is well known that for most of the past 2.5 billion years (since the Paleoproterozoic Era) environments, and their components, at Earth's surface have co-evolved with life and most of Earth's mineral diversity today may be a consequence, direct or indirect, of the biosphere (Hazen et al., 2008). Anyway, despite the effects of biosphere development at large scale are widely known and understood, the direct biota-rocks interactions at micrometric scale have been poorly studied for long. Although pioneering studies date back between the end of nineteenth and the beginning of twentieth century (cfr. Nadson, 1928), only in 1954 the term "Geomicrobiology" was coined, and defined as "the study of the relationship between the history of the Earth and microbial life upon it" (Beerstecher, 1954) as an evolution on Microbial Geology. Subsequently, Kuznetsov et al. (1963) defined it as "the study of microbial processes currently taking place in the modern sediments of various bodies of water, in ground waters circulating through sedimentary and igneous rocks, and in weathered Earth crust and also the physiology of specific microorganisms taking part in presently occurring geochemical processes". Such definition denote how the study of the interactions between biota and rocks was considered a part of other research fields like soil sciences, soil geochemistry and hydrogeochemistry. The systematic study of the interactions between biota and geosphere was born about 25 years ago when, among Microbial Ecology (as a branch of Life Sciences) and Microbial Biogeochemistry (as a branch of Earth Sciences), scientists started to consider Geomicrobiology as a separate science, more widely defined as "the role of microbes in geological processes, including mineral formation/deterioration, the cycle of elements and their chemical transformations" (Ehhrlich & Newman, 2008).

Previously, and in some ways still nowadays, the classical approach to this field of research clearly split the biological and the geological outcomes. The first are focused on the activities of microbes in transforming organic matter and inorganic substrates, the latest on the products of such activities (bio-mineralization) and the study of microbially influenced geochemical reactions and their kinetics, in order to reconstruct the cycling of inorganic and organic matter with an emphasis on environmental mass transfer and energy flow (Ehhrlich & Newman, 2008). For these reasons, the mineral-microbe reactions are called "the critical zone", which denotes the "heterogeneous, near-

surface environment in which complex interactions involving rock, soil, water, air, and living organisms regulate the natural habitat and determine the availability of life sustaining resources" (Konhauser et al., 2007).

In studying the processes involved in the critical zone it is necessary an interdisciplinary approach involving physical, chemical, geological and biological expertise. In particular, in approaching to biomaterials science, it is important to remember that bacteria, just like any other living being, carries out their activities in order to survive in the host environment. So every bio-mediated chemical reaction which happens at biota-mineral interface is functional to microbial sustain, it is energetically efficient, and driven by the basic assumption that it is carried out in order to modify the surrounding environment to more advantageous conditions. Great interest in microbial ecology, biochemistry and evolutionary biology studies arise from the consideration that microbes are ubiquitous and involved in almost all biosphere processes, suggesting that their evolution path yield them to develop particular ways of resistance allowing to adapt in living from mild to extreme environments, including highly polluted locations. A crucial point is their ability to survive to chemically and physically extreme environments, involving toxic elements in their life-cycle. In fact bacteria have the ability to fast adapt to new environmental conditions, developing resistance strategies which involve genetic expression of proteins suitable to manage and immobilize toxic elements. For these reasons many authors developed the idea that bacteria can be used for water and soils treatments in polluted areas in a process called "bioremediation", adding the business interest to the scientific research.

Regarding organic pollutants the bioremediation process consist in the bio-degradation of the organic matter or its transformation to non-dangerous species. In the bioremediation processes of toxic metals, obviously, their degradation is not possible, so there are two aspects of particular interest: 1) the ability of bacteria to modify the chemistry of a particular element and 2) their ability to immobilize it. The first point is quite critical when the polluting element is trapped in the polluted matrix and its removal proceed by means of chemical mobilization; the second one, on the opposite, allow to sink the polluting elements which are free to move in the matrix.

For all this reasons, the importance of bacteria in mineral precipitation is becoming increasingly appreciated in the geosciences. In literature has been reported that microbially mediated precipitation of geochemically relevant mineral phases (carbonates, sulfur-based minerals, metal-oxides, phosphates, ecc.) takes place in almost every environment on earth (Ehrlich & Newman, 2008; Kohnhauser, 2007) and, on the basis of some studies of microbial growth in the space, some authors suggest their presence in extraterrestrial systems (Russell et al., 1999; Nicholson et al., 2000; Cavicchioli, 2002).

Interest in bacterially promoted calcium carbonate precipitation has long existed, particularly in marine ecology, geochemistry and paleontology, due to the active role that play in the carbon cycle through biomineralization of carbonates. Calcareous biomineralization can occur through direct biological control of carbonate precipitation (and morphology) by organisms like shells and corals at macroscopic scale, and like coccoliths and foraminifera at microscopic scale, acting as structural or skeletal elements. Besides this, calcareous biomineralization can also occur passively through bacterially induced changes in system chemistry, as it happens in stromatolite structures which originate from special types of cyanobacterial mats, as result of deposition by entrapment and agglutination or by cyanobacterial photosynthesis (Pentecost, 1988). It is important to distinguish this process from active biomineralization, in which there is directed biological control on morphology, while in passive biomineralization carbonate precipitation is a "collateral effect" microbial activity. For these reasons such kind of mineralization typically appear as external crust onto bacterial cell walls, but in some cases mineral precipitation happens inside the microbial cells: they form $CaCO_3$ intracellularly and then export it to the cell surface to become support structures. Organisms that precipitate carbonates intracellularly and then export it to the cell surface include the coccolithophores (green algae) and foraminifera. The mineral phase of the calcium carbonate that is deposited is either calcite or aragonite (Lewin, 1965). Microbial carbonate precipitation has been observed, other than in marine environments, in soils, in lake, in freshwater and in thermal springs deposits (Konhauser et al., 2007). Calcium carbonate associated with travertine and lacustrine carbonate crusts and nodules can result from the photosynthetic activity of cyanobacteria in freshwater environments or from metabolic processes of other bacteria. Indeed, microbial carbonate precipitation as an important, widely diffused, geochemical process that is not a specific activity of any special group of bacteria. Actually, both heterotrophic and autotrophic bacteria, including sulfur bacteria, photosynthetic bacteria, chemo-bacteria, agar-, cellulose- and urea-hydrolyzing bacteria, nitrogen-fixing bacteria and sulfate-reducing bacteria have the ability to precipitate carbonates. This aspect is not surprising because it is quite easy to reproduce the optimal conditions for carbonate precipitation. In fact, because of the relative insolubility of carbonates, they are readily precipitated from aqueous solution at relatively low carbonate and cations concentrations; in particular Calcium carbonate, among the more common carbonates, has the lower solubility constant, with respect to the other carbonate phases as Mg- and Na- carbonates (Stumm & Morgan , 1981). Basically microbial precipitation of carbonates is based on the change of solution chemistry by adding or removing carbon dioxide, following the Le Chatelier principle in the carbonic acid dissociation reactions. Such chemical change could be reached in five main pathways:

1) Aerobic or anaerobic oxidation of carbon compounds consisting of carbon and hydrogen (carbohydrates, organic acids, hydrocarbons) producing CO_2 by means of respiration pathway in neutral or alkaline environments;

2) Aerobic or anaerobic oxidation of organic nitrogen compounds with the release of NH_3 and CO_2 in unbuffered environments containing sufficient amounts of calcium, magnesium, or other cations.

3) The reduction of $CaSO_4$ to CaS by sulfate-reducing bacteria using organic carbon as electron donor, thus producing CO_2.

4) The hydrolysis of urea leading to the formation of ammonium carbonate.

5) Removal of CO_2 from a bicarbonate-containing solution, which is the process used by photosynthetic microbes (as cyanobacteria, green, brown and red algae).

In any case, the basic conditions necessary for carbonate precipitations are the presence of sufficient amount of cations and carbonate at the optimal pH conditions. Because of these properties, carbonates precipitation is quite easy in many environments, especially for calcite which is particularly insoluble taking into account the Calcium concentration in marine and fresh waters.

Calcite is one of the most ubiquitous mineral in Earth's crust especially in sedimentary environments. Due to its fast kinetic in precipitation and dissolution and its crystalline structure, it is a geochemically and environmentally important mineral. Briefly, in the crystalline structure layers of Ca^{2+} atoms alternate with layers of $[CO_3^{2-}]$ groups along the c-axis. There is a single Ca^{2+} site, and its coordination environment is a trigonally elongated octahedron with each of the six Oxygen atoms at the corners belonging to a separate $[CO_3^{2-}]$ group. Due to its particular crystal structure it is well known that calcite is able to host in its crystalline lattice metal cations which substitute Calcium in the octahedral site and to accommodate structurally incompatible anions replacing carbonate oxyanion, thus acting as an efficient trap for potentially polluting elements (Elziga et al., 2002;).

Besides the merely passive uptake of metals and toxic elements in bio-mediated minerals, which could resemble the chemical uptake, the idea that bacteria could both regulate the geochemical cycle of an element (changing its chemical form and oxidation state) and induce the precipitation of a hosting mineral phase, it is an interesting perspective in the study of elemental cycling and in particular in its application to environmental sciences. Such point of view seems particularly critical for those elements which are difficult to sink in polluted environments due to their chemical properties (Warren et al., 2001; Dhami et al., 2013).

Given these premises, in this work our interest was focused on the study of bio-mediated uptake processes involving toxic elements which could be of huge treat for human health. Starting from previous works which regards areas affected by diffuse pollution, we decided to focus on Arsenic.

Such choice was driven by two main considerations: 1) it is well known that many bacteria are able to resist and carry on their living processes using Arsenic as electron donor and/or acceptor, and 2) Arsenic is a toxic element ubiquitous in Earth Crust which has very different geochemical behavior on the basis of its speciation as a consequence of environmental conditions, influencing its sink into geological traps.

Regarding the first point, there are a number of microorganisms that directly reduce As^{V} to As^{III}, using fermentation products as their electron donors (Oremland and Stolz, 2003). Up until now, however, none of know species are obligate Arsenate reducers. In fact, they all naturally respire using more efficient electron acceptors (as Fe^{III}, Nitrogen compounds, Sulfates, Oxygen,…) but are able to switch to dissimilatory Arsenate reduction when their preferred substrates are unavailable (Laverman et al., 1995). Regarding the reduction process, recent studies have highlighted the presence of a highly conserved pair of membrane proteins (ArrA and ArrB) that form a dedicated complex for Arsenate respiratory reduction. These genes are present in virtually every As^{V}-respiring bacterium isolated, regardless of the phylogenetic placement of the bacterium (Malasarn et al., 2004; Silver & Phung, 2005). In addition to the dissimilatory respiration process, many common microorganisms (e.g., *E. coli, B. subtilis*) are able to reduce As^{V} by means of detoxification process. Such species possess a different suite of genes that specifically encode for As^{V} reduction via a cytoplasmic Arsenate-reductase (ArsB and ArsC), followed by As^{III} removal from the cell by means of a chain of reactions pathway (Cervantes et al., 1994).

Regarding the second point, it is well known that in Earth's crust Arsenic is mainly present, especially in groundwater systems, in the trivalent (As^{III}) and pentavalent (As^{V}) inorganic forms. Among a different toxicity (As^{III} compounds are more toxic than As^{V} ones) these two forms have different geochemical behavior which influences their attitude to sink, and thus their bioavailability. The oxidized form, Arsenate, easily adsorb onto mineral surfaces (especially, iron and aluminum oxy-hydroxides, calcite and micas), which can limit its hydrological mobility. On the contrary, Arsenite adsorbs less readily to mineral surfaces, making it the more mobile oxyanion (Dixit et al., 2003; Sø et al., 2008).

The occurrence of Arsenic in groundwater and soils can derive from either anthropogenic (such as mining activities; cfr. Costagliola et al., 2008) or natural sources. Usually, the natural occurrence of arsenic in groundwater is related to the presence of geothermal systems (Angelone et al., 2008) or from the water–rock interactions that lead to arsenic mobilization from the aquifer, both in reducing and oxidizing environments, under specific geochemical and stratigraphical conditions (Smedley and Kinniburgh 2002). In Italy, many occurrences of high arsenic concentrations have been related to volcanic regions as the Bullicame Hot Springs, close to Cimini Volcanic complex, in the Roman

Magmatic Province (Angelone et al., 2008; Di Benedetto et al., 2011) and in mining areas such as the Pecora River Valley in Southern Tuscany (Costagliola et al., 2010).

The worldwide attention is focused on the acute and chronic long-term health effects observed in populations exposed to arsenic-rich drinking waters, in fact from epidemiological studies it seems that arsenic can cause a number of different illnesses (skin, lung, and bladder cancer; cfr. Yoshida et al., 2004). Because of these reasons, in Europe Arsenic concentrations in drinking waters and soils is ruled by a severe legislative quality standards (98/83 EC Directive 1998), fixing the maximum allowable concentration at 10 μg/L (the previous limit was 50 μg/L) for drinking waters, while for soils ranges from 20 to 50 mg/kg depending on the destination of use.

At the same time, it is well know that there are a lot of geological traps which can sink Arsenic, reducing its bioavailability and thus the risk for human health. A lot of studies pointed out how Arsenic is easily trapped in some minerals by absorption onto the mineral surface or by co-precipitation. Again Arsenic speciation highly influences these processes: in fact As^{V} in solution is present as arsenic acid which is a strong acid and it is already dissociated at neutral or slightly alkaline pH. On the other hand, As^{III} is present as arsenious acid which is a weak acid and dissociates only at highly alkaline pH (Sø et al., 2008; Yokoyama et al., 2012). This means that arsenious acid has no charge and it is unlikely to link to mineral surface, reducing or, at most, preventing adsorption and/or co-precipitation process.

Both the adsorption and co-precipitation processes have been demonstrated to be efficient for Arsenic removal from a solutions, but depending on the mineral surface properties it has different applications and efficiency. In fact, many authors studied the As removal by means of metal-oxide (in particular Iron-oxide), observing that the process is quite efficient, but at the same time Arsenic adsorbed onto mineral surface is suitable to be released if the chemistry of solution changes (Dixit et al., 2003; Aredes et al., 2012; Luther et al., 2012). On the other hand, many studies on natural travertines have pointed out that calcite precipitation is a very efficient process for Arsenic sink (Di Benedetto et al., 2011; Winkel et al., 2013). Differently from surface adsorption, uptake in calcite seems to be a more stable trap because Arsenic precipitates during calcite growth and it is host inside the crystalline lattice. In such way it is not concentrated only onto the mineral surface and it is less allowable to be removed till calcite is not dissolved.

Nevertheless, trace element incorporation in calcite is controlled by the detailed structure of the mineral surface, which varies spatially on different faces, as well as with external conditions. Consequently, despite chemical or biological controls can affect the whole process at large scale, in the understanding of the Arsenic uptake process in calcite we cannot neglect the interactions between the As-oxyanions in solution and the mineral surface during calcite precipitation. In order

to investigate in depth the uptake process it is necessary an approach which consider only the mineral surface instead of the bulk. Surface sciences allow to concentrate only on the interfacial environment, yielding more detailed insights about the atomic-scale structures, including absorption and incorporation processes. The main tools for surface detections are scanning probe microscopies (e.g. atomic force microscopy) and electron-based techniques (e.g. XPS) and X-ray Reflectivity techniques. Recent developments in surface sciences have pointed on techniques which can be applied to surfaces in contact with water, allowing to measure mineral-fluid interface structures *in situ* for direct insight into the geochemical phenomena of interest resembling the real conditions. In fact it is improper to assume that a mineral surface can be removed from an aqueous solution without modifying its surface structure (Fenter, 2002). The use of X-ray techniques is ideal for probing of mineral-water interfaces at atomic scale because they readily penetrate relatively thick volumes of water allowing to investigate the mineral-water interface *in situ*, and X-rays can measure atomic scale structures because of their wavelengths which are commensurate to atomic size. X-ray Reflectivity (XR) techniques measure the angular distribution of X-rays scattered elastically from a surface or an interface and are derived from the same theoretical foundation as X-ray crystallography, which is widely used to study the bulk crystalline structures. The idea of XR techniques is to provide both qualitative and quantitative data concerning the arrangements of atoms at mineral-fluid interface (e.g., atomic locations, bond lengths) with sub-Ångstrom precision. In particular specular XR techniques yield a structural reconstruction along the surface normal direction, while lateral structures are probed by non-specular reflectivity.

Because the uptake of any trace element onto a mineral passes through its surface, XR analysis of Arsenic uptake in calcite could yield more detailed insight in understanding how the process takes place. In particular the techniques is suitable to settle down how arsenic interacts at the mineral-water interphase, and subsequently if it is incorporated and if it orders inside the calcite crystalline lattice during calcite epitaxial growth process.

Finally, we decided to employ X-Ray Reflectivity techniques to investigate the Mercury uptake process in calcite too. Such idea arise from two main considerations: 1) Mercury is another pollutant element, dangerous for human health, whose diffusion in the environment is still in part poorly understood and 2) Hg^{2+} ionic radius is quite similar to Ca^{2+}, so it is possible to suggest a substitution into calcite crystalline lattice. With this in mind and considering that in polluted areas Mercury can be mobilized in groundwater and spread on wide areas, the perspective to sink it in a common and stable mineral phase could be an environmentally interesting process. Despite this, up to now no systematic studies about Mercury trapping in calcite has been carried out, so we purpose

to understand the uptake process from the basic interactions of the ion in solution at the mineral-water surface.

Part 1: Arsenic uptake in bacterial calcite

INTRODUCTION

Arsenic is a ubiquitous trace element on the Earth crust (Smedley and Kinniburgh, 2002). High geogenic concentration of this element are often associated with sulphide ore deposits and geothermal areas (Acharyya et al., 1999; Costagliola et al., 2008; Costagliola et al., 2010; Elziga et al., 2002) whereas the most relevant human activities prompting As in the food chain are mining, metal smelting, combustion of fossil fuels, agricultural pesticide, use and production of timber treatments (Matschullat, 2000; Smedley and Kinninburg, 2002; WHO 2010). Adsorption of arsenic by Fe- and Mn-oxyhydroxide surfaces is considered among the most important and widespread mechanisms controlling As mobility. The destabilization of these phases, or the desorption of As oxyanions from their surfaces, is considered one of the most effective pathways to the human food chain and of concern about the human health (Nriagu, 1994; Lenoble et al., 2002; Sherman and Randall, 2003; Dixit and Hering, 2003; Ouvrard et al., 2005; Tufano et al., 2008).

Recently, a growing number of papers (cf. Winkel et al., 2013 and reference therein) have been devoted to As trapping in the calcite structure, after the pioneering papers of Cheng et al. (1999) and Di Benedetto et al. (2006). Arsenic (As) bearing calcite is in fact considered a more stable sink for As since, in principle, is less sensitive to surface exchange reactions with respect to Fe-Mn oxyhydroxides (Bardelli et al., 2011). Given its diffusion in many geologic environments, calcite is believed to compete, in regards to As mobility, with Fe-Mn oxyhydroxides, as it was already observed for many other elements substituting Ca in the octahedral site (Elziga et al., 2002; Fenter & Sturchio, 2004; Catalano et al., 2008; Fenter et al, 2008; Fenter & Sturchio, 2012).

The incorporation of As in the calcite crystalline lattice follows the substitution of [$AsO3^{3-}$] after [$CO3^{2-}$] (Di Benedetto et al., (2006),)determining a partial distortion of the lattice, due to the different steric properties of the anions involved, that triggers an expansion along the c-axis (Cheng et al., 1999; Roman-Ross et al., 2006; Bardelli et al., 2011).

Currently there is no general agreement about the mechanism for the substitution reaction. Sø et al., (2008), Alexandratos et al., (2007) and Yokoyama et al., (2012) claimed that almost only As^{V} anions, which in addition are the most abundant in groundwater and oxygenated environments, are incorporated in calcite. Sø et al. (2008) explained such an effect on the basis of the different chemical behaviour of Arsenate and Arsenite in solution: from mildly basic to highly basic pH, arsenious acid is almost not dissociated in solution, retaining a zero-charge, and so it's unable to adsorb onto the calcite surface during the calcium carbonate precipitation process. On the contrary, arsenic acid, that is a stronger acid than arsenious acid, is present in dissociated form even at relatively low pH forming a negative oxyanion that makes it able to adsorb onto (positively charged) calcite surface. This finding has been further confirmed by Yokoyama et al. (2012) which

precipitated calcite in presence of solutions containing both As^{III} and As^{V} showing that almost only As^{V} is adsorbed and incorporated in calcite. Natural As-bearing calcite generally conform to the laboratory results (Bardelli et al., 2011; Costagliola et al., 2013; Winkel et al., 2013) mainly containing As^{V} but some notable exception are known. In particular, Di Benedetto et al. (2006) and Bardelli et al., (2011) on the base of EPR and XAS spectroscopies, found that natural calcite from travertine deposits of Central Italy prevalently hosts As^{V} but may indeed contain some As^{III}.

Bardelli et al., (2011), although speculatively, argued that bacteria could have played some role in favouring the uptake of As^{III} in the calcite lattice since it's widely known that the calcite formation process is greatly influenced by bacteria and algae which populate many environments (e.g. lakes and hot springs; Warren et al., 2001; Perito and Mastromei, 2011; Achal et al., 2012). Bacteria are, in addition, able to participate to the biogeochemical cycle of elements, especially those with various oxidation states, which can be used as electron donors/acceptors (Konhauser, 2007) to support several metabolic pathways for energy production (Oremland & Stolz, 2003; Lloyd & Oremland, 2005). These reactions, in the case of As^{III} – As^{V} redox couple, demonstrated to regulate the As-cycling in lakes (Mono Lake, USA; Oremland et al., 2003), in mine wastes and in water saturated anaerobic soils (Weisener et al., 2011; Corsini et al., 2010). Moreover, evidence for As-bearing bacterial calcite is reported in the very recent literature (Achal et al., 2012).

The aim of this work was to investigate the role of bacteria in As trapping processes during calcium carbonate precipitation. We have chosen the Bullicame hot springs in the northern Latium magmatic province (Italy) as a model environment, where deep hot waters enriched in As (Angelone et al., 2009) reach the surface, precipitating travertines which contain variable amounts of As (39-279 ppm) which is prevalently bound (about 95%) to calcite (Ciardi et al., 2011). Among bacteria isolated from the Bullicame hot waters, we selected one strain for its calcite precipitation ability in presence of As. Biogenic and synthetic calcite obtained in presence of As were then compared by means of XRD, XRF and XAS analysis. Moreover, we explored if and how the calcite chemistry can affect the As uptake by adding Mg to the solution where calcite was grown.

EXPERIMENTAL

Sampling area

The thermal area of Viterbo (Northern Latium, Central Italy) is composed by several hot springs ("Carletti Pool", "Zitelle", "Bagnaccio", "Masse di San Sisto" and "Bullicame") all located in a small and well defined area (Fig. 1), usually referred as the "Bullicame" thermal field (Di Benedetto et al., 2011). The physical and chemical properties of the water at Bullicame, as well as

the mineralogical and chemical characteristics of the travertine precipitated by the thermal waters, have been described in detail by Di Benedetto et al. (2011) and Angelone et al., (2009). The hot springs contain variable amounts of As generally clustering around 300-400 ppb (Angelone et al., 2009) but unfiltered water samples may reach higher As content (up to 1 ppm) depending on the (arsenical)-calcite particulate abundance. All the hot springs show clear signs of biological activity with microbial mats and biofilms onto and below the surface of new-forming travertines.

Water sampling, bacteria isolation and identification

Two water samples from the hot spring Bullicame, one near the edge and the other near the center of the spring, were collected into sterile glass bottles and immediately brought to the laboratory. At the spring, water had a temperature of 57°C, a pH of 6.5 and a conductivity of 2.75 mS. Each water sample was filtered through 0.2 µm Millipore filter; then the microbial cells trapped onto filter were collected by washing filters with the filtered water. Small volumes (0.1 mL) of undiluted and serially diluted cell suspensions were plated on Nutrient Agar (NA, OXOID) As-enriched (As-en NA) by adding to the medium 1/10 volume as Bullicame filtered water, and incubated up to two weeks at 57°C. Growing colonies were observed at the stereomicroscope and classified on morphology. For each morphotype, some strains were streaked and then isolated on As-en NA.

The selected strain BD5 (see RESULTS), was identified by means of rDNA analysis. Genomic DNA extraction, PCR conditions, purification and sequencing of the amplified 16S rDNA were carried out as described in Marvasi et al. (2009). Sequences were assembled and edited with Chromas software; highly similar sequences were searched by BLAST at the NCBI database (http://www.ncbi.nlm.nih.gov). The newly generated 16S sequence of strain BD5 was deposited at the Genbank database.

Bacterial calcite precipitation

Calcite production by the isolated bacterial strains was tested in the B4 precipitation growth medium (0.4% yeast-extract, 0.5% dextrose, 0.25% calcium acetate, 1.5% agar if solid, buffered at pH 8). Bacillus subtilis 168 was used as calcite producing control strain (Barabesi et al. 2007). Strains able to make precipitates were then streaked in the B4 As-enriched medium obtained by progressively adding a filter sterilised As solution (H_3AsO_4 standard solution 1000 ppm [Merk]) to B4 up to 10 ppm (As-enB4).

All the subsequent analysis on bacterial calcite were carried out on carbonates produced by the

selected strain called BD5 (see Results) in As-enB4 medium added with As 10 ppm.

Bacterial cultures in As-enB4 were incubated at 57°C for 2 weeks on solid and to 4 weeks in liquid medium. Calcite production was monitored visually by observing cthe growth of calcite crystals in solution and through a stereomicroscope on solid medium. At the end of the incubation period, crystals from solid culture media were collected by scraping the bacterial streaks from plates and washing them several times in distilled water until the suspension appeared clear. Liquid cultures were similarly clarified by several washing steps. Then suspensions were filtered on Whatman grade 5 cellulose filters and subsequently dried. Carbonate samples BR2 and BR5 were obtained from BD5 culture in As-enB4 solid and liquid medium, respectively.

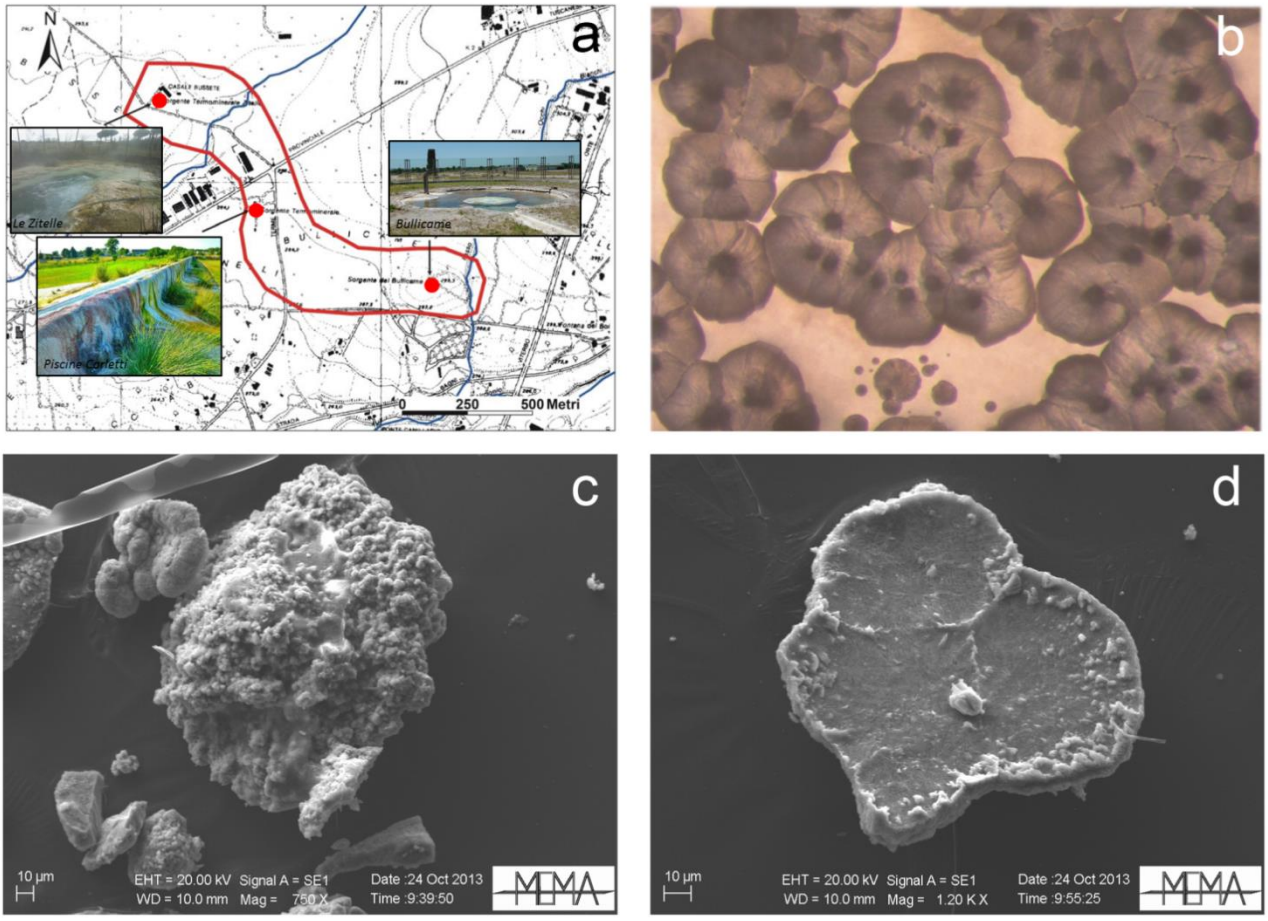

Fig.1 – Location of Bullicame Hot Springs (a). Calcite crystals produced by *B. licheniformis*, BD5 streaked on solid medium: crystals embedded into the BD5 streak observed at the stereomicroscope 57X (b) and SEM-SE imaging of isolated calcite concretions (c and d)

In order to investigate if the Mg-Ca substitution in calcite octahedral site could induce a lattice modification which positively affects the As uptake in the calcite, As-enB4 medium was modified adding Mg (by means of Mg-acetate) maintaining the Mg/Ca molar ratio slightly below 2% to

prevent dolomite precipitation. Carbonate samples BR1 and BR4 were obtained from BD5 culture in Mg enriched As-enB4 solid and liquid medium, respectively.

Moreover, an As-free and Mg-free standard sample (namely BR6) was produced growing BD5 in unmodified B4 medium. All the details about bacterial carbonate samples are reported in Tab.1a.

Bacterial calcite samples were analyzed by Scanning Electron Microscopy (SEM) imaging (ZEISS EVO MA15) in order to investigate their morphology, texture and crystallinity (Fig.1).

In order to better appreciate the calcite development onto bacterial cells, we cultured strain BD5 (see Results) up to 30 hours of incubation in liquid As-enB4 medium in bottles where sterile flat cleaved inorganic calcite crystals at the bottom were used as a substrate for bacterial growth (Fig.2).

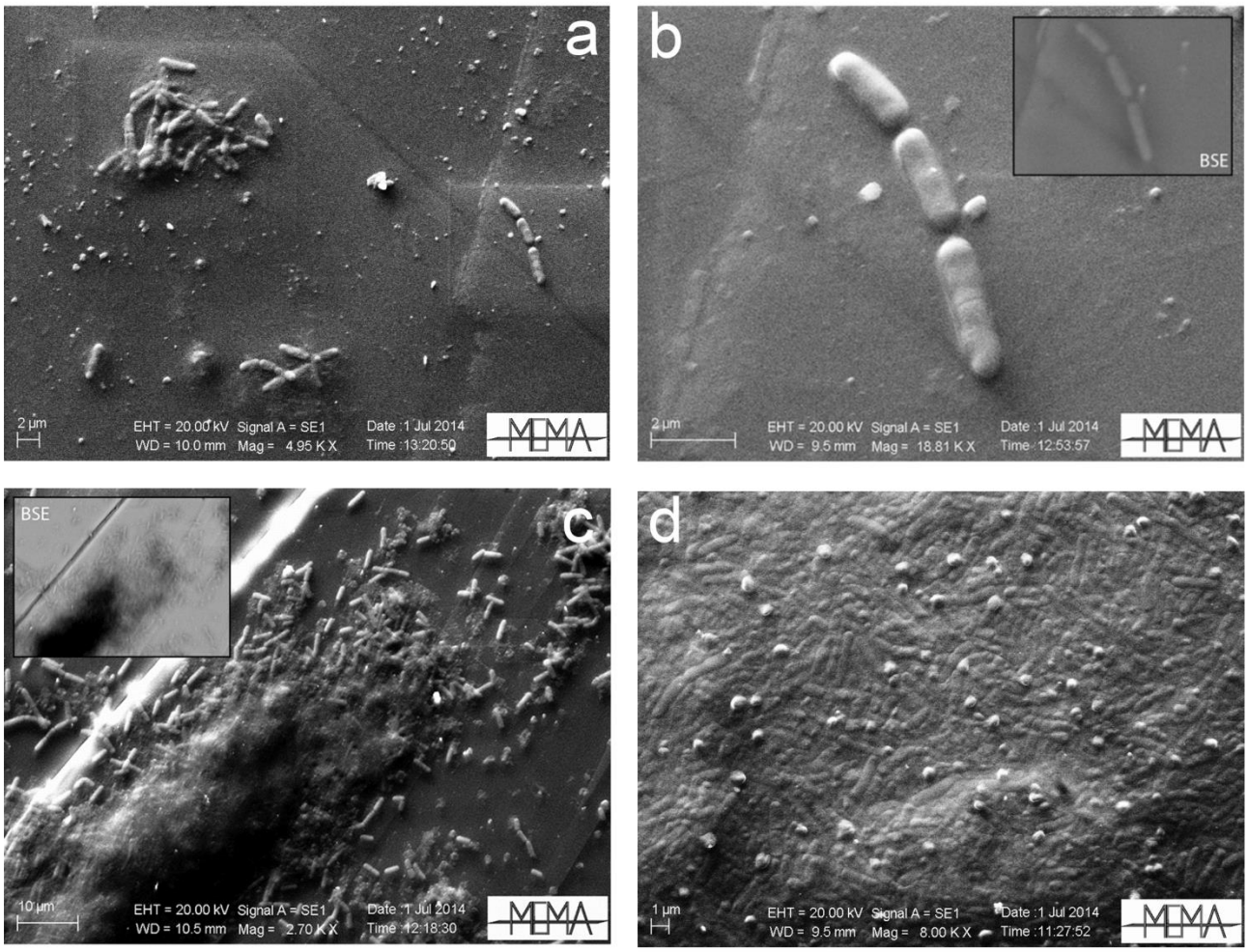

Fig. 2 – *B. licheniformis* BD5 growth and calcite production onto inorganic calcite surface in liquid medium observed at SEM: after 3hr of incubation (a), bacterial cells appear in short chains and small aggregates adherent to the surface. A detail of 2a, showing a short chain of three rod cells (in the inset the SEM-BSE imaging; b); after 7hr of incubation, bacterial biofilm more developed. The SEM-BSE image shown in the inset underlies the wide extracellular polymeric matrix (black area); after 30 hr of incubation, the bacterial mat completely covers the inorganic surface, several endospores are visible (white dots).

Reference material collection, production and analysis

A set of reference calcite samples was prepared for comparison purposes.

The first one was prepared collecting both fossil and presently-forming travertines. Fossil travertines were sampled at the Bullicame area (samples BL4, BL5, BL7) and in the Pecora Valley district (Southern Tuscany, Italy; cfr. Costagliola et al., 2010; Bardelli et al., 2011; sample TRSE). Presently forming travertines were all sampled at Bullicame Hot Springs (samples BL1, BL2, BL3, ZIT).

A second set of reference samples was prepared precipitating abiotic As-bearing calcite (samples RR3, RR5 and RR5Mg2) following the procedure by Roman-Ross et al. (2006). Briefly, the abiotic calcite was precipitated mixing 100 ml solution 0.5M Na_2CO_3, 1mM As (~75 mg/L), buffered at pH 8.9 with NaOH, with a solution 0.5M $CaCl_2$, added drop by drop for 1h, while stirring. Magnesian calcite was produced adding both 0.5M $CaCl_2$ and $MgCl_2$ solutions, maintaining Mg/Ca molar ratio <2%. Sodium Arsenate dibasic hepta-hydrate, $Na_2HAsO_4*7H_2O$ (Sigma Aldrich), and arsenious acid, H_3AsO_3, in nitric acid solution 0.1N (Merk) were used as As source for As^V (RR5, RR5Mg), and As^{III} (RR3), respectively. In order to avoid any As^{III} oxidation, the As^{III}-bearing calcite RR3 was precipitated in an oxygen-free chamber (O_2 < 1ppm).

Arsenic extraction from travertines and synthetic calcite was obtained by acid dissolution of 0.5 mg of ball-milled sample in "aqua regia" ($HCl+HNO_3$) and 1h mineralization in microwave oven (CEM Mars-5 microwave mineralizer). The arsenic concentration was determined by means of Inductively Copuled Plasma – Optical Emission Spectroscopy (ICP-OES) analysis (Perkin Elmer Optima 8000). A complete list of the reference samples and their details are reported in Tab. Ib.

XRD, XRF and XAS measurements

Biological calcite samples, after washing and milling, were analyzed for their mineralogical composition by XRD. Because of the slight amount of biological calcite produced by bacterial cultures, As concentration in biogenic calcites was carried out by means of XRF – instead of ICP-OES – in order to preserve material for further analyses. XAS and XRF samples were prepared in the same way: biogenic calcites were milled and pressed in 3mm thick punched plastic holders and enclosed with 0.2 mm thick polyimide film tape.

X-Ray Diffraction (XRD)

XRD measurements were performed with Philips PW 1050/37 X-ray powder diffractometer (Earth Sciences Dept., University of Florence), operating with a Cu anode, a graphite monochromator and

with a PANalytical X'Pert PRO data acquiring system. A thin layer of milled biogenic carbonates was applied on a silicon wafer in order to get spectra with a low background. Each spectrum was recorded from 8° to 120°, with a spacing of 0.2° measured for 0.1 sec. Yttrium oxide (Y_2O_3) was used as reference material. All the spectra were analyzed with GSAS-EXPGUI (Toby, 2001) software in order to get refined cell parameters and phase amounts (weight %).

X-Ray Fluorescence (XRF)

XRF measurements were performed with WD-XRF Rigaku PrimusII (CRIST – Structural Crystalchemistry Interdepartmental Center, University of Florence), equipped with a Rh X ray source and Silicon monochromator. The X-ray spot size suitable for measurements ranges from 0.5 to 30 mm, but because of the small amount of biogenic carbonates we were allowed to prepare samples with a surface area about 2x4 mm and thus to perform measurements at maximum with 1 mm spot size.

As reference material for instrument calibration were used some travertines from Bullicame Hot Springs (Tab. Ib), previously analysed by means of ICP-OES to get As concentration. Such samples ranges from 10 to 206 ppm in an essentially $CaCO_3$ matrix. Because some of our samples were out of this scale, eight standard samples were produced mixing As_2O_5 (Merk) and $CaCO_3$ (Merk) and measured in the same way, to calibrate the instrument in the range 300 - 3000 ppm As.

X-Ray Absorption Spectroscopy (XAS)

Bulk XAS experiments on the As K-edge at the GeoSoilEnviroCARS bending magnet beamline 13-BM-D were performed at 13-BMD beamline at the Advanced Photon Source (APS), Argonne National Laboratory (ANL - Argonne, IL). The K -edge XANES spectra were collected in fluorescence mode from -150 to 640 eV with 5 eV steps before the main edge (11871.5 eV for As^V; 11868 eV for As^{III}), and across the main edge (from -15 eV to 25 eV) with 0.25 eV steps, controlled with a Si(111) monochromator. Samples were held between polyimide film tape in punched Plexiglas holders (as described above), mounted in the X-ray beam at a 45° angle. X-ray fluorescence was recorded using a 19 element Ge solid-state array multi-element detector and the incident beam intensity (I_0) was recorded using a standard ionization detector. Energy calibration was performed by assigning the K -edge energy of As^V (11871.5 eV) and As^{III} (11868 eV) of some standard materials: Arsenic Oxide (As_2O_5), scorodite ($Fe^{3+}AsO_4 \cdot 2H_2O$) and schneiderhöhnite ($Fe^{2+}Fe^{3+}{}_3[As_5O_{13}]$), Arsenious Oxide ($As_2O_3$), Calcium Arsenate ($Ca_3(AsO_4)_2$) and Sodium Arsenate ($Na_2HAsO_4 \cdot 7H_2O$). Depending on the XRF and ICP-OES results, and the quality of the spectra recorded, a different number of scans was performed on each sample: at least 3 for higher

As-bearing samples (BR4, BR5) to at most 12 in the case of lower-As (RR3). Such scans were then merged and averaged to increase the intensity to noise ratio. Data DT correction and analysis was performed with Athena XAS data processing software, Demeter Pack (Ravel & Newville, 2005).

RESULTS

Isolation and characterization of bacteria from Bullicame Hot Springs

Bacterial colonies grown from Bullicame water belonged to different morphotypes by means of optical microscopy observation. More strains as representatives of each morphotype were selected for a total of 65 strains and tested for their calcium carbonate precipitation capability. The strains showing faster growth and appreciable amounts of precipitates were sequentially selected by streaking them on As-enB4 medium with increasing amount of H_3AsO_4 up to 10 ppm. In the end we decided to concentrate for further investigation only on one strain, called BD5, which showed the best precipitation potential (Fig.1) and was further characterized by PCR amplifying and sequencing its 16S rDNA. Sequence analysis showed a 97% identity with the 16S rDNA of *Bacillus licheniformis*. BD5 cell morphology, a rod spore-forming bacterium as observed at the optical microscope and at SEM (Fig.2), fitted with the molecular classification. Calcite produced by BD5 on solid As-enB4 forms crusts reaching a size of about 200 micrometer. SEM imaging allowed us to observe that these crusts are composed by a fine-grained aggregate of calcite, without any appreciable crystalline structure (Fig.1).

Table Ia – List of biological carbonates produced by *B. licheniformis* and As concentration (XRF)

Sample	Description	Growth medium	As (mg/kg)	As solution (mg/L)	Kd (L/kg) $[As]_{SOL}/[As]_{LIQ}$
BR1	Biogenic, solid culture medium Mg/Ca <2%	As-en B4	43	~10	4,3
BR2	Biogenic, solid culture medium	As-en B4	27	~10	2,7
BR4	Biogenic, liquid culture medium Mg/Ca <2%	As-en B4	1381	~10	138
BR5	Biogenic, liquid culture medium	As-en B4	1053	~10	105
BR6	Biogenic Calcite, solid culture medium	B4	-	-	-

The production of calcite during bacterial growth onto inorganic calcite surface was observed at different time by SEM up to 30 hours of incubation (Fig. 2d). After 3 hours of incubation, BD5

bacterial cells appeared in short chains and small aggregates deposited onto the inorganic calcite surface (Fig. 2a). In the following hours the bacterial biofilm progressively developed up to cover the whole calcite surface producing a more thick extracellular polymeric substance (EPS) matrix entrapping cells (Fig. 2c-d). By SEM-BSE images, bacterial cells appeared covered by a calcite envelope since after 3h of cultivation, as shown by the low compositional contrast with the calcite support (Fig. 2b). The developing of thick biofilms is appreciable by the presence of a wide dark area on the bright calcite substrate (Fig. 2c).

Table Ib – List of reference materials and their As concentration (ICP-OES).

Sample	Description	As (mg/kg)	As solution (mg/L)	Kd (L/kg) $[As]_{CAL}/[As]_{LIQ}$
BL1	Now-forming travertine, Bullicame (VT), Italy	154	~1	154
BL2	//	206	~1	206
BL3	//	201	~1	201
BL4	Fossil travertine, Bullicame (VT), Italy	160	~1	160
BL5	//	185	~1	185
BL7	//	123	~1	123
ZIT	Travertine Zitelle Hot Spring (VT) Italy	91	0.58	157
TRSE	Fossil travertine, Pecora River Valley, Italy	110	-	-
RR5	Synthetic calcite	169	74.9	2.2
RR5Mg	Synthetic calcite, Mg 2%	419	74.9	5.6
RR3	Synthetic calcite	2.3	74.9	0.03

XRD

XRD analyses have revealed that the biogenic carbonates produced in liquid culture are actually composed by a mixture of calcite and vaterite, whereas carbonates precipitated in a solid culture are mainly made of calcite. The amount of vaterite, calculated by means of Rietveld analysis is about 8% in BR4 and 40% in BR5 (Tab. II). The biogenic carbonates BR1 and BR2, produced in the solid growth medium, in addition to the calcite XRD pattern exhibit a weak but distinct peak at about 3.5 Å, which doesn't match with any $CaCO_3$ polymorph. Finally, XRD spectra didn't show any Mg-phase in appreciable quantities in any sample.

Regarding cell reticular constants, results reported in Tab. II clearly indicate that biogenic calcite in BR4 and BR5 (produced in liquid media), containing a relevant amount of As (see below), exhibit a

larger cell constants and volume. The c-axe values – 17.0910 Å and 17.0988 Å respectively – are about 0.02-0.03 Å longer than the other bacterial calcite samples. In fact, calcite in BR2 owns reticular constants fully comparable (17.0664 Å) with those reported for calcite in literature (cfr. Graf, 1961; Markgraf & Reeder, 1985) and the As-free BR6 (17.0765 Å), while BR1 exhibit a shorter c axe: 17.0506 Å. Finally, it's worthwhile to note that biogenic magnesian calcites (BR1 and BR4) exhibit shorter c-axes of their equivalent Mg-free samples BR2 and BR5.

Table II – Mineralogical composition and refined reticular constants of biological calcite.

Sample	Phases	Phase ratio (wt %)	Calcite reticular constants (Å)			Cell volume (Å^3)
			a	c	c/a	
BR1 (Mg)	calcite	-	4.9765 (0.0001)	17.0506 (0.0006)	3.426	365.709 (0.023)
BR2	calcite	-	4.9848 (0.0002)	17.0664 (0.0007)	3.424	367.253 (0.032)
BR4 (Mg)	calcite vaterite	91.7% 8.3%	4 .9903 (0.0004)	17.0910 (0.0014)	3.425	368.597 (0.072)
BR5	calcite vaterite	60.8% 39.2%	4.9916 (0.0005)	17.0988 (0.0022)	3.425	368.951 (0.077)
BR6	calcite	-	4.9858 (0.0001)	17.0765 (0.0009)	3.425	367.63 (0.02)
Calcite (Markgraf & Reeder, 1985)			4.988	17.061	3.420	367.6

XRF

XRF measurements performed on the biogenic carbonates and the reference materials are reported in Tab.Ib. Bio-calcite produced in solid culture-media have respectively 27 (BR2) and 43 (BR1) mg/kg of As, against the 1053 (BR5) and 1381 (BR4) mg/kg of the samples produced in the liquid one, despite the initial As concentration in the growth medium was the same (10 ppm). The calcite froming the travertines from Bullicame Hot Springs and Pecora Valley exhibit As concentration ranging from 91 mg/kg to 206 mg/kg.

As regards the apparent distribution coefficient, Kd (L/kg), calculated as the ratio between arsenic concentration in the whole precipitate (composed by calcite and vaterite in BR4 and BR5) against that in the initial solution (cf., Yokoyama et al., 2012), we found a value of about 10^2 (138 and 105, respectively) for bio-calcite produced in the liquid culture media. Similar Kd values we found for travertines at the Bullicame Hot Springs: in such springs As concentrations in the thermal waters range from 300 ppb to 1 ppm, from 91 to 206 mg/kg in travertines, with ($123<Kd<206$). As regards bacterial calcite produced in the solid As-enB4 culture media (BR1 and BR2) Kd are much lower: 2.7 and 4.3 respectively.

It is stressed that the samples BR4 and BR5 show variable amounts of vaterite (about 40wt % in BR5 and 8wt% in BR4), which is not negligible in the estimation of apparent Kd for calcite. Notwithstanding this, the two samples, that were prepared following the same procedure (liquid As-enB4 culture media) show comparable amount of As and Kd values.

XAS

Arsenic K-edge XANES spectra of As-bearing bio-carbonates, travertines, synthetic calcite and the other reference materials are reported in Fig. 3a and Fig. 3b.

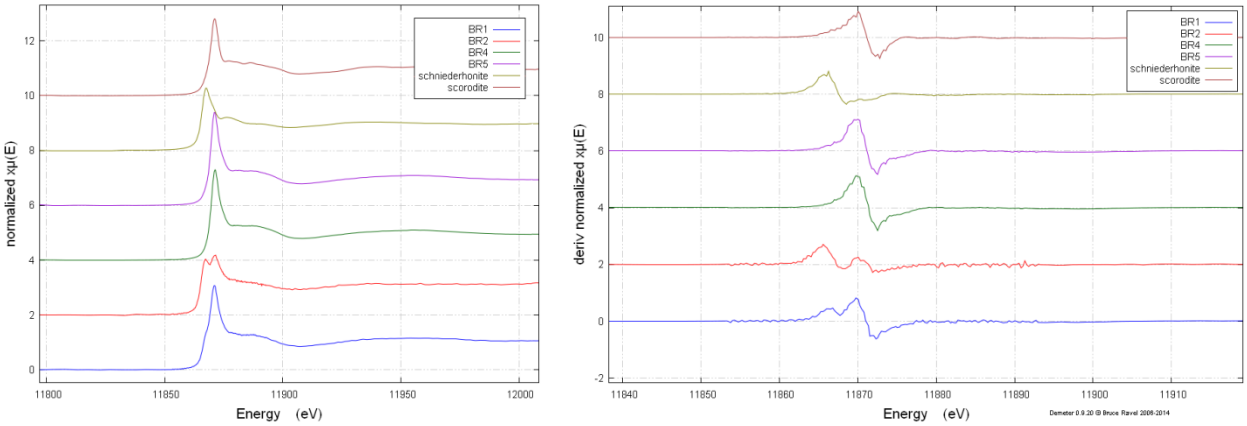

Fig. 3 – XAS K-edge absorption spectra of bacterial calcite samples cultured both in liquid and solid culture medium compared with two standard samples for As^{V} (scorodite) and As^{III} (schneiderhonite) (a) and derivative functions of the same spectra (b).

From Fig.3a and Fig.3b, where XANES spectra are compared with two standard materials (scorodite, $Fe^{3+}AsO_4 \cdot 2H_2O$ and schneiderhöhnite, $Fe^{2+}Fe^{3+}{}_3As_5O_{13}$), it could be observed that biogenic samples produce different spectra as a consequence of their culture medium (liquid or solid). Samples BR4 and BR5, both from liquid culture medium, exhibit only the absorption edge of As^{V}. On the contrary, biogenic samples produced in a solid culture media (BR1, BR2) contain, instead, both As^{V} and As^{III}. This feature is evidenced in Fig. 4 where are reported the BR1 and BR2 deconvoluted spectra fitted by means of linear combination of two standard's spectra: schneiderhöhnite for As^{III}, and scorodite for As^{V}. Such linear combination roughly indicate that the ratio As^{III}/As^{V} in biogenic carbonates is about 1:4 for BR1 and 2:1 for BR2. The same spectra treatment and calculation has been carried out for sample RR3, an abiotic calcite with As^{III}, obtaining a As^{III}/As^{V} ratio of about 2:1.

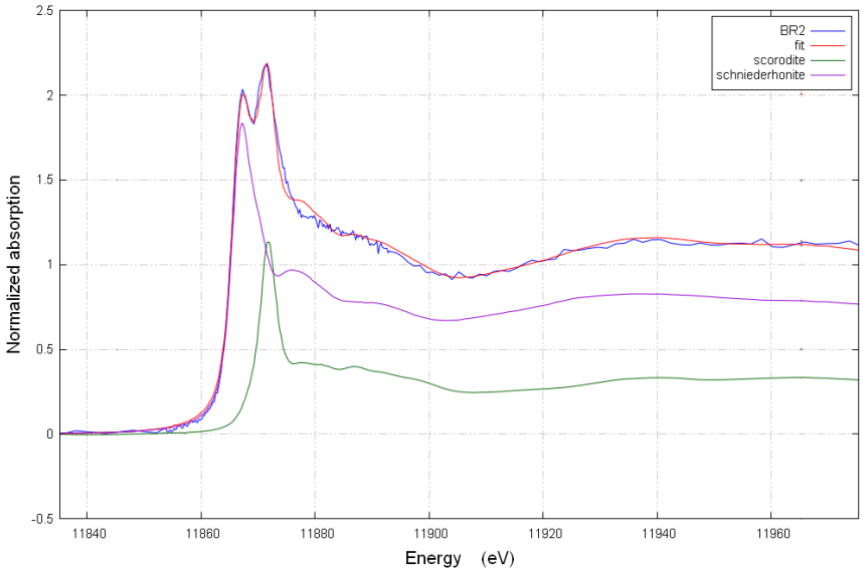

Fig. 4 – Linear square fit of BR2 XAS spectrum (blue) using a linear combination of the scorodite (green) and schneiderhonite (violet) spectra.

As comparison, some natural As-bearing travertines were analyzed: both the now-forming and fossil Bullicame Hot Spring travertines exhibit only the As^{V} absorption edge in the XANES region, similarly to biogenic samples produced in liquid culture media, and none of them shows a pattern similar to BR1 and BR2. Other than the arsenic oxidation state, the similarities between BR4 and BR5, and Bullicame travertines are evident in EXAFS region (Fig 5a), which is diagnostic to understand if As is adsorbed or co-precipitated with calcite (Winkler et al., 2013).

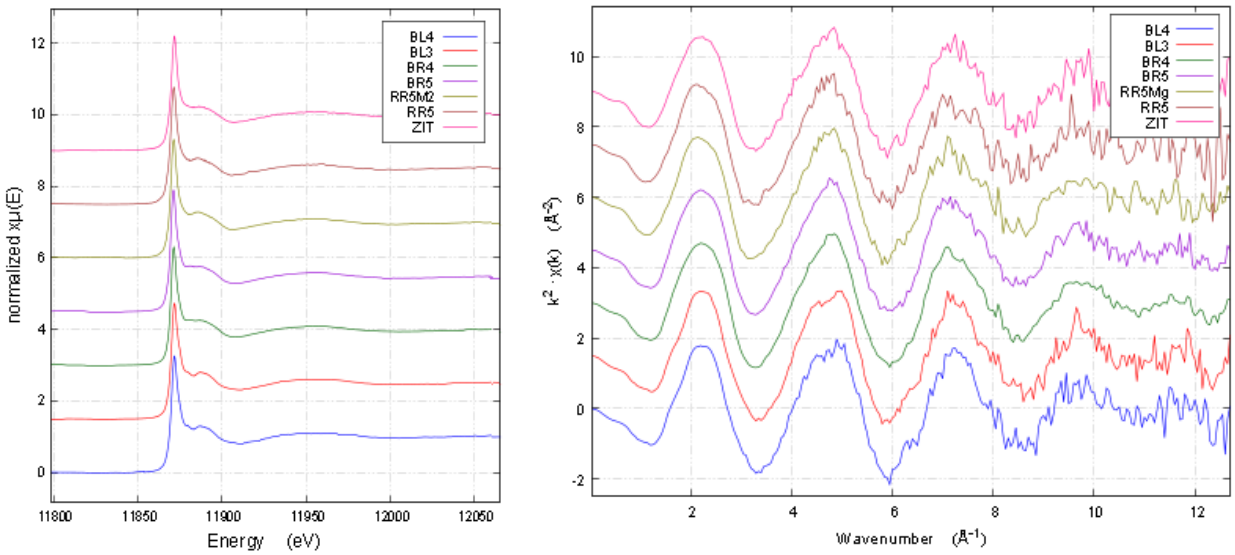

Fig. 5 – XAS spectra at the Arsenic K-edge (a) and k-space converted XAS (b) of bacterial calcites precipitated from liquid medium (green, violet) compared with Bullicame Hot Springs Travertines (blue, red, pink) and synthetic calcites (brown, light green)

Substantially As^V-bearing calcite samples could be divided in two main groups: in the first case a broad band occur close to the As^V K absorption edge (11871.5 eV), while in the other case a shoulder is present at about +8eV and two feature at +15 eV and +20 eV, respectively. ZIT and TRSE travertines (from Zitelle Hot Spring and Pecora Valley, respectively; Tab.II) belong to the first group, having a spectrum very similar to the abiotic calcites RR5 and RR5Mg2. The Bullicame travertines (here only BL3 and BL4 are reported; Fig.5a-b) exhibit the features of the second group, just like the other travertines from Bullicame Hot Spring (spectra not reported). Finally, the biogenic calcite BR4 and BR5 have intermediate spectra: in fact they exhibit a weak feature close to the absorption edge, similar to the shoulder in the travertines spectra, but also a broad band in the region +15eV and +20eV (Fig 4.a). Such features are much more evident in k-space converted EXAFS spectra (Fig. 5b): in fact Bullicame travertines (BL) exhibit a clear split of the 4.8 $Å^{-1}$ band and a small shoulder at 6.3 $Å^{-1}$, while ZIT, TRSE, synthetic calcites (RR5 and RR5Mg2) and biogenic calcites (BR4 and BR5) exhibit a single frequency oscillation without any particular feature.

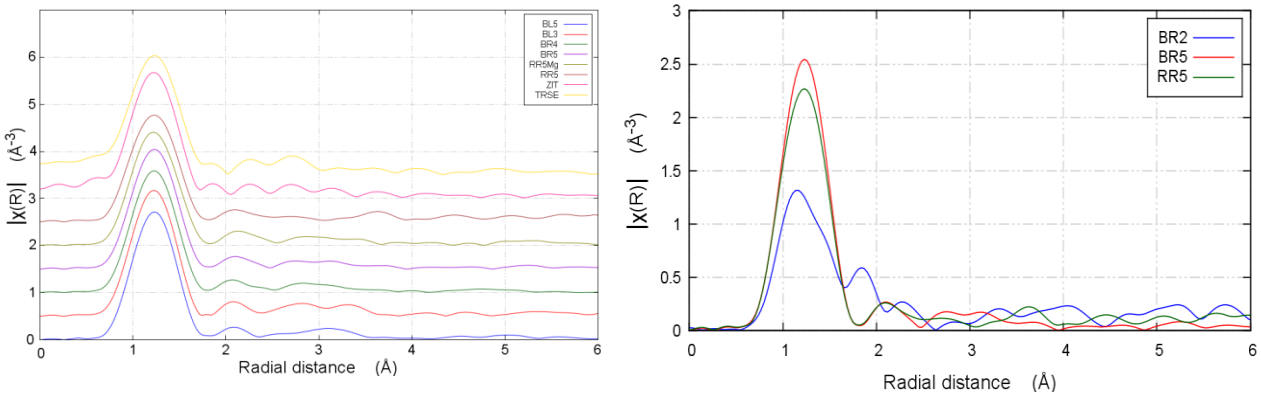

Fig. 6 – R-space converted spectra As^V bearing samples (a) of bacterial calcites precipitated from liquid medium (green, violet) compared with Bullicame Hot Springs and Pecora River Valley Travertines (blue, red, pink, yellow) and synthetic calcites (brown, light green) and AsIII bearing BR2 compared with As^V bearing BR5 bacterial calcite and RR5 synthetic calcite.

Finally, from EXAFS in R-space (Fig. 6a) it is clear that in all the spectra there are low or negligible peaks at R>2 Å (values not corrected for phase shift). Finally, the BR2 biogenic calcite exhibits an R-space EXAFS spectrum with a clear combination of peaks in the range 1Å < R < 2Å, corresponding to different first coordination shells for the two the different oxidation state As^{III} and As^V (Fig. 6b).

DISCUSSION

Data on As trapping during calcite precipitation by bacteria reported in this work come from a study on strain BD5 of *B. licheniformis* isolated from the Bullicame hot spring. *B. licheniformis* is a spore-forming bacterium commonly found in soil and with a high potential for biotechnological applications (Veith et al. 2004). Strain BD5 resulted able to fast precipitate calcite in a suitable medium (calcite was present onto bacterial cell surface after 3 h of cultivation, Fig. 2) entrapping both As^{III} and As^{V} in the growing calcite.

Our results clearly indicate that the nature (liquid vs solid) of the bacterial growing media greatly influences the experimental results. Concerning mineralogy, solid medium favors the precipitation of calcite with slight amount of other phases, whereas liquid medium triggers the precipitation of both calcite and vaterite. This result is not surprising since it is known that vaterite is a common product of the biological activity during carbonate precipitation from liquid solutions (Warren et al., 2001; Achal et al., 2012). Yokoyama et al., (2012) observed that, under abiotic conditions, a low percentage (at most 5%) of vaterite was present during calcite precipitation from supersaturated solution in the pH range 9-11, and the amount of such polymorph decreases with aging of the sample until 54h, when all the vaterite disappeared. Ogino et al., 1987, reported in fact that vaterite is a metastable early phase, precursor of calcite, during its precipitation from $CaCO_3$ highly supersaturated solutions. Because vaterite is a labile phase at ambient temperature and pressure conditions, it's gradually transformed into calcite, which is the stable $CaCO_3$ polymorph.

It is reported in literature that the vaterite/calcite conversion may be hindered by the presence of cations in the precipitating solution (cfr. Kamiya et al., 2004) as well as Arsenic oxyanions as described by Yokoyama et al. (2012) which attribute this phenomena to the As surface sorption process which is thought to inhibit the vaterite-calcite transformation, increasing the vaterite lifetime. In our samples the amount of vaterite (up to almost 40% in BR5) is certainly higher than those reported by Yokoyama et al. (2012) and Achal et al. (2012). Moreover considering that in the present study the biological samples in the liquid culture media were produced in 4 weeks, our results suggest that under high As concentrations, like those adopted in our experiments, the biological process of $CaCO_3$ precipitation extends the vaterite lifetime with respect to abiotic $CaCO_3$ precipitation.

It is not known if a critical concentration of As which inhibits the vaterite-calcite transformation exists, but Winkel et al. (2013) reported of travertines with ~1000 mg/kg Arsenic, precipitated from solutions containing 3700 ppb Arsenic, with no evidence of vaterite. Equally, travertines from the Bullicame area, even the new-forming ones showing evident signs of biological activity, are mainly

made up by calcite with minor aragonite occurrence (Di Benedetto et al., 2011). Such comparison suggests that an extended aging under ambient conditions allows a continuous vaterite-calcite transition.

In order to assess the effectiveness of bio-mediated process, the As Kd (L/kg) was adopted as discriminating parameter to evaluate the As uptake by calcite. From the results reported above, it could be observed that commensurate As concentrations and values of Kd are obtained for the biogenic calcite prepared in a liquid medium and those observed at Bullicame. Conversely, the concentration of As in calcite samples produced on solid medium is much lower with Kd remarkably lower than those observed for the Bullicame travertines. Since the initial concentration of As in the two growing media was the same (10 ppm), the straightforward explanation of this difference in concentration could be the different diffusion and availability of As in the two growth media (liquid vs solid). More in detail, in the liquid media, the diffusion of As is conceivably rapid enough to replenish the depletion produced by the As uptake from calcite and/or vaterite growing onto the bacterial cells, but the same process could be hindered in the solid medium.

Besides this, our results denote another interesting insight: a low amount of Mg in the growth media highly increases the uptake of As^{V} from the solution. Namely, regarding biogenic samples, we clearly observed an increase of As in both the solid and liquid culture media Mg-bearing BR1 and BR4 of about 59% and 33% with respect to the Mg-free BR2 and BR5. In the abiotic sample (RR5) this trend is clearly confirmed. Such effect of Mg in the As uptake was not yet studied although in the patented arsenical calcite (US patent 8227378; cfr. Costagliola et al., 2014) the inventors suggest to prepare calcite adding some Mg without specifying the specific effect of Mg in the As uptake.

The positive effect (higher Kd) of Mg on the As uptake could be explained considering the steric effect of the Mg-Ca substitution in the calcite lattice, which causes the shrinking of the octahedral site. This outcome may contribute to better accommodate the As oxyanions replacing the carbonate group (cf. Bardelli et al., 2011). More precisely, the Arsenite and Arsenate anions have larger steric clearance than the carbonate group. As a consequence, if arsenic oxyanions substitute for the carbonate planar group, the calcite lattice adapts extending the c axis (Cheng et al., 1999; Bardelli et al., 2011 and reference therein) and the Mg^{2+} (0.72 Å) substitution for Ca^{2+} (0.99 Å), since the smaller ionic radius of the former, could better accommodate the c-axis stretching.

XRD results confirm such picture since bio calcites with higher amount of arsenic (BR4 and BR5) clearly exhibit elongated cell constants, which is consistent with literature suggestion about the elongation of c-axe due to the pyramidal shape of Arsenite and tetrahedral Arsenate instead of planar carbonate group (Cheng et al., 1999; Roman-Ross et al., 2006; Di Benedetto et al., 2011).

Accordingly, it's clear that biogenic calcite with low As contents (e.g. BR2) shows reticular constants similar to non-biogenic As free calcite (Markgraf & Reeder, 1985) and biogenic As-free calcite BR6, suggesting that c-axe expansion doesn't work for low As concentrations. On the contrary, for relatively high As concentrations (samples BR4 and BR5) such effect is significant with an increase of the c-axe length in As-bearing calcite of ~0.03 Å with respect to As free calcite. Comparing such results with literature, similar c-axe values were found by Di Benedetto et al. (2011) for Bullicame Travertines (Carletti Pool) calcite, suggesting strong similarities between these materials, among the similar Kds. On the contrary, Winkel et al. (2013) didn't found any increase in c-axe elongation in travertine samples, despite As concentrations up to 900 ppm, so it could be possible that the amount of As is not the only factor which regulates the length of reticular constants. Some authors (Pokroy et al., 2006; Zolotoyabko et al., 2010) reported that biogenic calcite own elongated c-axes explaining this effect with the presence of interlayered bio-molecules in calcite lattice. Because biogenic calcites contain organic matter, this could be a crucial factor other than As amount, even if none of such studies reported c-axe values commensurate with Bullicame travertines and biogenic calcites. Finally, an opposite, weaker effect seems linked to Mg: in fact, Mg-bearing calcites BR1 and BR4 have correspondingly shorter c-axes than Mg-free BR2 and BR5. Such effect could be related to the shorter ionic radius of Mg (0.72 Å) with respect to Ca (0.99 Å), in agreement with literature (Paquette & Reeder, 1990).

XAS data seem to indicate that the Bullicame travertines, and synthetic and biogenic carbonates produced in liquid culture media contain exclusively As^{V}. This evidence confirms the results obtained by several authors in the recent literature (e.g., So et al., 2008, Yokoyama et al., 2012, Alexandratos et al., 2007; Bardelli et al., 2011) although Bardelli et al., (2011) report the presence of As^{III} oxyanions in travertine samples from the Pecora River Valley (Southern Tuscany, Italy). Noteworthy, the As K-edge XANES analysis clearly indicate that biological carbonates precipitated from solid culture media host As^{III} in addition to As^{V}. This result is extremely interesting because the As introduced in the culture media was only As^{V} and all the bacteria cultures and measurements on the biogenic products were carried out in aerobic conditions, so it's clear that a reduction process occurred during incubation.

It seems clear that, because the As^{III}/As^{V} oxidation/reduction potential ranges from +60 to +135mV (Lloyd & Oremland, 2005), the As^{V} reduction to As^{III} was performed by bacteria. It is well known that bacteria can reduce Arsenate following two main pathways: 1) the dissimilatory Arsenate reduction to As^{III} carried out by some bacteria able to respire Arsenate coupling the reaction with the oxidation of organic matter; 2) the Arsenate reduction pathway to As^{III} via the ArsC system, which is a mechanism of detoxification and resistance. The Arsenate reductases involved in these

two pathways are different (Silver & Phung, 2005; Oremland & Stolz, 2003). *B. licheniformis* is known to possess genes encoding ArsC (Corsini et al., 2010), while in literature there are no evidences about its ability to perform the Arsenate dissimulative reduction. For this reason, our discussion will be focused on ArsC-mediated As reduction.

Arsenate reduction linked to detoxification processes is well explained in the literature (Silver & Phung, 2005; Oremland & Stolz, 2003; Lloyd & Oremland, 2006). Briefly, Arsenate chemically mimic phosphate and it's allowed to enter the microbial cell by the pathways designated for phosphate uptake, interfering with phosphate-based biochemical pathways (e.g. oxidative phosphorylation). Bacteria developed a particular resistance to As which consists in the reduction of As^{V} to As^{III} with a specific cytoplasmatic protein ArsC (Arsenate reductase). Once the arsenic is reduced it is no more able to mimic phosphate and it's suitable to be excreted out of the cell via ArsB-type, an As^{III} -specific transport proteins (Silver & Phung, 2005; Oremland & Stolz, 2003).

In order to explain how As^{III} uptake in calcite could take place, first of all it's worth to notice that As^{III} is present only in bacterial calcite produced by *B. licheniformis* on solid growth medium. It is conceivable that *B. licheniformis* reduces As^{V} to As^{III} by means of the ArsC pathway when it grows in solid as well as in liquid medium. The fate of As^{III} can however be different in liquid and solid medium, due mainly to two factors: rate of diffusion and biofilm structure.

We have already argued that liquid medium allows for faster diffusion of As^{V} (causing a higher As concentration in precipitated calcite) than the solid one; the same could be for As^{III} and oxygen. In the liquid medium, as long as floating bacteria reduce As^{V} to As^{III}, the availability of As^{III} and O_2 could be high enough to let re-oxidizidation of As^{III} to As^{V} eventually occurs. This could explain the absence of As^{III} in calcite bacterially precipitated in liquid medium (BR4 and BR5), as well as in Bullicame Travertines.

On solid medium, in addition to the reduced diffusion of arsenic and oxygen into the medium, we have to consider that bacteria grow onto the surface where they are streaked, forming quite quickly an external thick biofilm (at solid-air interface). Biofilm would work as a barrier hindering not only the oxygen from air to penetrate, but also As^{III}, available at the bacterial cell surface by ArsB-mediated excretion, to move out of the biofilm-air interface. Here As^{III} can concentrate and eventually be entrapped into the growing calcite inside the bacterial biofilm.

The mechanism we propose for As uptake by bacteria in the growing calcite in liquid and solid medium is showed in the picture in Fig. 7. As^{III} uptake in calcite seems then to be possible only in particular conditions, in which low diffusion of As and O_2 is allowed. Comparing bacterial calcite with natural travertines, we assume that the liquid culture media samples BR4 and BR5 should resemble an hot spring environment with a continuous groundwater supply and relatively high fO_2,

like Bullicame Hot Springs or the other ones reported in literature (e.g. Winkler et al., 2013). On the contrary, low diffusion conditions, as described above for the solid culture medium (samples BR1 and BR2) likely resemble a wetland environment; this could be the case of Pecora Valley River travertines which are mainly made up of "lacustrine and phytoclastic travertines" (Costagliola et al. 2010).

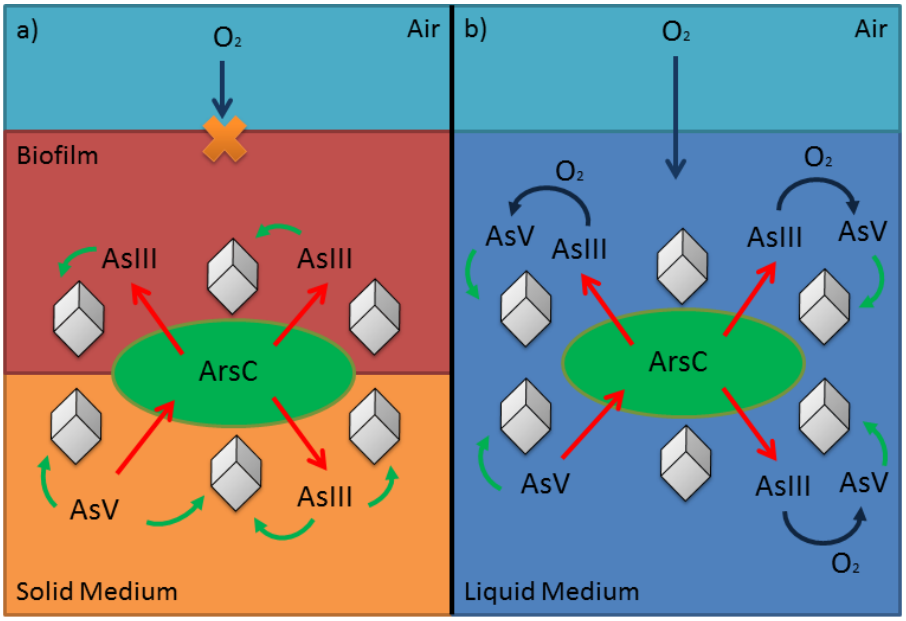

Fig.7 – Schematic picture of the supposed Arsenic uptake process in solid (a) and liquid (b) medium

Regarding the arsenic uptake process in calcite, XAS data yield us useful insights. Our results clearly show that all the samples own a distinct first-shell coordination (1.23Å without phase shift correction), which corresponds to the As-O bonds of the Arsenate (estimated 1.69 Å). On the contrary, despite EXAFS spectra exhibit some slight differences in the R-space region from 2 to 6 Å, there's no evidence of a second coordination shell. Such effect has been observed by Winkler et al. (2013) and Bardelli et al. (2011) for travertines, and it has been explained as a result of low atomic ordering in the second shell of coordination of As, "suggesting a poor crystalline structure of adsorbate" (Bardelli et al., 2011). The same authors suggested how EXAFS features in the spectral region close to the As K edge could yield useful clues about the As uptake processes, allowing to distinguish if As is adsorbed onto calcite surface or it is co-precipitated with calcite.

Comparing our results (Fig. 5) with those reported by Winkler et al. (2013) it seems clear that in Bullicame travertines co-precipitation of As in calcite is prevalent, while in ZIT and TRSE travertines, just like synthetic calcites RR5 and RR5Mg, absorption onto mineral surface seems to be prevalent. Biogenic calcite BR4 and BR5 have an intermediate pattern, suggesting a commensurate effect of the two uptake processes, with prevalent absorption. In any case, all the

samples show almost similar k-space spectra (Fig. 5b), suggesting slight differences in the second shell coordination, and they "have an almost single-frequency oscillation reflecting in a single well defined peak in the real (R) space. This means that virtually no contributions from coordination shells higher than the first" (Bardelli et al., 2011). Such results clearly indicate that in all the samples As is low ordered out of the Arsenate coordination oxygens (Fig. 6a). As regards the As^{III}-bearing biogenic samples, BR1 XAS spectrum is very similar to travertines, because of the low As^{III}/As^{V}, while BR2 has a complex R-space EXAFS spectrum, due to the presence of As with different oxidation state, and consequently different first coordination shells. Differently from As^{III}-bearing travertines reported by Bardelli et al. (2011), there's no evidence of second shell coordination in the region from 3 to 6 Å, suggesting a low crystalline ordering also for Arsenite (Fig.6b).

Finally, XAS data show that in none of the analyzed samples there's an As ordering in calcite lattice, independently from the precipitation process and As oxidation state. Such results allow us to figure out that As uptake in biogenic calcite is, in some way, similar to the process which allows As^{V} uptake in travertines and abiotic calcite (involving both co-precipitation and adsorption processes), but at the same time it clearly allows As^{III} to sink despite thermodynamic considerations presented by other authors (So et al., 2008, Yokoyama et al., 2012). Stated this, we suppose that in bacterial biofilms particular environmental conditions, namely high-pH, are reached, causing deprotonation of arsenious acid and thus its adsorption onto the positively charged bio-calcite surfaces. Alternatively, the action of organic ligands could be argued to explain the As^{III} uptake by calcite.

CONCLUSIONS

A multi-methodological characterization was performed on biogenic calcites produced by the As-resistant bacterium *B. licheniformis*, combining SEM imaging, X-ray Diffraction (XRD), X-ray Fluorescence (XRF), and X-ray Absorption Spectroscopy (XAS), in order to investigate the bio-mediated As uptake in calcite and point out the critical factors of this process.

The culturing medium has been noted to be a critical factor which strongly affects the phase composition of the biogenic products, the amount of As trapped in calcite and its oxidation state. In particular, our results suggest that the low diffusion in the solid medium hinder the diffusion of As, reflecting in a lower apparent distribution coefficient, Kd (L/kg), and oxygen, allowing the presence of Arsenite in the precipitated calcite, starting from an As^{V}-bearing solution.

This last issue is probably the most interesting outcome of this work. In fact it is known about the

ability of bacteria to reduce As^{V} to As^{III} (Silver & Phung, 2005; Oremland & Stolz, 2003) and to precipitate calcite (Achal et al., 2012), as long as the ability of calcite to sink As^{V} (Winkel et al., 2013), but our results clearly demonstrate that the biogenic process could produce As^{III}-bearing calcite. Arsenite uptake in calcite has been widely debated in literature (Cheng et al., 1999; Roman-Ross et al., 2006; Di Benedetto et al., 2006), but up until now no clear evidence has been reported in literature, with the only exception of Pecora Valley travertines reported by Bardelli et al. (2011), who argued about the possible role of bacteria in Arsenite uptake in natural travertines. Our findings clearly confirm such theory.

Finally, our results suggest quite clearly that the presence of Mg during calcite precipitation positively affects As uptake in calcite both in the chemical and bio-mediated process. Despite this aspect goes beyond the aims of this work, our findings lead us to figure that As uptake induce a lattice distortion, reflecting in the elongation of c-axes, as asserted for first by Cheng et al. (1999), while Mg induce a shrinking due to its lower ionic radius. Such sort of "compensation" seems to positively affect As uptake in calcite, suggesting the use of Mg for As removal by calcite in biotechnological applications.

References

Achal V., X. Pan, Q. Fu, D. Zhang (2012) Biomineralization based remediation of As(III) contaminated soil by Sporosarcina ginsengisoli. *Journal of Hazardous Materials* 201-202: 178-184

Acharyya SK, Chakraborty P, Lahiri S, Raymahashay BC, Guha S, Bhowmik A (1999) Arsenic poisoning in the Ganges delta. *Nature* 401: 545

Alexandratos V.G., E.J. Elziga, R.J. Reeder (2007) Arsenate uptake by calcite: Macroscopic and spectroscopic characterization of adsorption and incorporation mechanisms. *Geochimica et Cosmochimica Acta* 71: 4172–4187

Angelone M., C. Cremisini, V. Piscopo, M. Proposito, Fabio Spaziani (2009) Influence of hydrostratigraphy and structural setting on the arsenic occurrence in groundwater of the Cimino-Vico volcanic area (central Italy). *Hydrogeology Journal* 17: 901–914

Barabesi C., A. Galizzi, G. Mastromei, M. Rossi, E. Tamburini, and B. Perito. 2007. *Bacillus subtilis* Gene Cluster Involved in Calcium Carbonate Biomineralization. *Journal of Bacteriology* 189 (1): 228-235.

Bardelli F., M. Benvenuti, P. Costagliola, F. Di Benedetto, P. Lattanzi, C. Meneghini, M. Romanelli, L. Valenzano (2011) Arsenic uptake by natural calcite: An XAS study. *Geochimica et Cosmochimica Acta* 75: 3011–3023

Catalano J.G., C. Park, P. Fenter, Z. Zhang (2008) Simultaneous inner- and outer-sphere Arsenate adsorption on corundum and hematite *Geochimica et Cosmochimica Acta* 72(8): 1986-2004

Cheng L., P. Fenter, N.C. Sturchio, Z. Zhong, M.J. Bedzyk (1999) X-ray standing wave study of Arsenite incorporation at the calcite surface *Geochimica et Cosmochimica Acta* 63(19/20): 3153–3157

Corsini A., L. Cavalca, L. Crippa, P. Zaccheo, V. Andreoni (2010) Impact of glucose on microbial community of a soil containing pyrite cinders: Role of bacteria in arsenic mobilization under submerged condition. *Soil Biology & Biochemistry* 42: 699-707

Costagliola P., F. Bardelli, M. Benvenuti, F. Di Benedetto, P. Lattanzi, M. Romanelli, M. Paolieri, V. Rimondi, G. Vaggelli (2013) Arsenic-Bearing Calcite in Natural Travertines: Evidence from Sequential Extraction, μXAS, and μXRF. *Environmental Science & Technology* 47: 6231−6238

Costagliola P., M. Benvenuti, L. Chiarantini, S. Bianchi, F. Di Benedetto, M. Paolieri, L. Rossato (2008) Impact of ancient metal smelting on arsenic pollution in the Pecora River Valley, Southern Tuscany, Italy. *Applied Geochemistry* 23(5): 1241-1259

Costagliola P., M.M. Benvenuti, M.G. Benvenuti, F. Di Benedetto, P. Lattanzi (2010) Quaternary sediment geochemistry as a proxy for toxic element source: A case study of arsenic in the Pecora Valley (southern Tuscany, Italy) *Chemical Geology* 270(1–4): 80-89

Dhami N.K., M.S. Reddy, A. Mukherjee (2013) Biomineralization of calcium carbonates and their engineered applications: a review. *Frontiers in Microbiology* 4: 1-13

Di Benedetto F., P. Costagliola, M. Benvenuti, P. Lattanzi, M. Romanelli, G. Tanelli (2006) Arsenic incorporation in natural calcite lattice: Evidence from electron spin echo spectroscopy. *Earth and Planetary Science Letters* 246: 458 – 465

Di Benedetto F., G. Montegrossi , A. Minissale, L.A. Pardi, M. Romanelli, F. Tassi, A. Delgado Huertas, E.M. Pampin, O. Vaselli, D. Borrini (2011) Biotic and inorganic control on travertine deposition at Bullicame 3 spring (Viterbo, Italy): A multidisciplinary approach. *Geochimica et Cosmochimica Acta* 75: 4441–4455

Elziga E. J. and R. J. Reeder (2002) X-ray absorption spectroscopy study of Cu2+ and Zn2+ adsorption complexes at the calcite surface: Implications for site-specific metal incorporation preferences during calcite crystal growth. *Geochimica et Cosmochimica Acta* 66(22): 3943–3954

Fenter P., P. Geissebühler, E. DiMasi, G. Srajer, L.B. Sorensen, N. C. Sturchio (1999) Surface speciation of calcite observed in situ by high-resolution X-ray reflectivity. *Geochimica et Cosmochimica Acta* 64(7): 1221–1228

Fenter P., N.C. Sturchio (2004) Mineral–water interfacial structures revealed by synchrotron X-ray scattering. *Progress in Surface Science* 77: 171–258

Fenter P., Neil C. Sturchio (2012) Calcite (104) – water interface structure, revisited. *Geochimica et Cosmochimica Acta* 97: 58–69

Fukushi K., M. Sakai, T. Munemoto (2011) Arsenic sorbent for remediating arsenic-contaminated material. US Patent No: 8,227,378

Kamiya N., H. Kagi, F. Tsunomori, H. Tsuno, K. Notsu (2004) Effect of trace lanthanum ion on dissolution and crystal growth of calcium carbonate. *Journal of Crystal Growth* 267: 635645.

Lloyd J.R. and R.S. Oremland (2006) Microbial Transformations of Arsenic in the Environment: From Soda Lakes to Aquifers. *Elements* 2: 85-90

Markgraf S.A., R.J. Reeder (1985) High-temperature structure refinements of calcite and magnesite *American Mineralogist* 70: 590-600

Marvasi M., E. Vedovato, C. Balsamo, A. Macherelli, L. Dei, G. Mastromei, and B. Perito. 2009. Bacterial community analysis on the Mediaeval stained glass window "Natività" in the Florence Cathedral. *Journal of Cultural Heritage* 10:24-133.

Ogino T., T. Suzuki and K. Sawada (1987) The formation and transformation mechanism of calcium carbonate in water. *Geochimica et Cosmochimica Acta* 51: 2757–2767.

Oremland R.S, J.F. Stolz, J.T. Hollibaugh (2004) The microbial arsenic cycle in Mono Lake, California *FEMS Microbiology Ecology* 48 (2004) 15–27

Oremland R.S. and J.F. Stolz (2003) The Ecology of Arsenic. *Science* Vol. 300: 939–944

Paquette J., R.J. Reeder (1990) Single-crystal X-ray structure refinements of two biogenic magnesian calcite crystals. *American Mineralogist* 75: 1151-1158

Perito B., G. Mastromei (2011) Molecular Basis of Bacterial Calcium Carbonate Precipitation. In: *Molecular Biomineralization, Aquatic Organisms Forming Extraordinary Materials*. Müller W.E.G. ed., Springer-Verlag Berlin Heidelberg, pp. 113-139.

Pokroy B., A.N. Fitch, F. Marin, M. Kapon, N. Adir, E. Zolotoyabko (2006) Anisotropic lattice distortions in biogenic calcite induced by intra-crystalline organic molecules. *Journal of Structural Biology* 155: 96–103

Ravel B. & M. Newville (2005) ATHENA, ARTEMIS, HEPHAESTUS: data analysis for X-ray absorption spectroscopy using IFEFFIT. *Journal of Synchrotron Radiation* 12: 537–541 doi:10.1107/S0909049505012719

Román-Ross G., G.J. Cuello, X. Turrillas, A. Fernández-Martínez, L. Charlet (2006) Arsenite sorption and co-precipitation with calcite. *Chemical Geology* 233: 328 – 336

Silver S. and Phung Le T. (2005) Genes and Enzymes Involved in Bacterial Oxidation and Reduction of Inorganic Arsenic. *Applied and Environmental Microbiology* 71(2): 599–608

Smedley P.L., D.G. Kinniburgh, (2002) A review of the source, behaviour and distribution of arsenic in natural waters *Applied Geochemistry* 217: 517–568.

Sø H.U., D. Postma, R. Jakobsen, F. Larsen (2008) Sorption and desorption of Arsenate and Arsenite on calcite. *Geochimica et Cosmochimica Acta* 72: 5871–5884

Toby B. H. (2001) EXPGUI, a graphical user interface for GSAS. *Journal of Applied Crystallography* 34: 210-213

Veith, B., Herzberg, C., Steckel, S., Feesche, J., Maurer, K. H., Ehrenreich, P., Bäumer, S., Henne, A., Liesegang, H., Merkl, R., Ehrenreich, A., Gottschalk, G. (2004) The complete genome sequence of *Bacillus licheniformis* DSM13, an organism with great industrial potential. *Journal of Molecular Microbiology and Biotechnology* 7(4):204-211

Warren L.A., P.A. Maurice, N. Parmar, F. Ferris (2001) Microbially mediated Calcium Carbonate precipitation: Implications for interpreting calcite precipitation and for solid-phase capture of inorganic contaminants. *Geomicrobiology Journal* 18(1): 93-115

Weisener C.G., J.W. Guthrie, C.M. Smeaton, D. Paktunc, B.J. Fryer (2011) The effect of Ca–Fe–As coatings on microbial leaching of metals in arsenic bearing mine waste *Journal of Geochemical Exploration* 110: 23–30

Winkel L.H.E., B. Casentini, F. Bardelli, A. Voegelin, N.P. Nikolaidis, L. Charlet (2013) Speciation of arsenic in Greek travertines: Co-precipitation of Arsenate with calcite. *Geochimica et Cosmochimica Acta* 106: 99–110

Yokoyama Y., K. Tanaka, Y. Takahashi (2012) Differences in the immobilization of Arsenite and Arsenate by calcite. *Geochimica et Cosmochimica Acta* 91: 202–219

Part 2: Arsenic and Mercury uptake onto calcite(104) surface: preliminary results from a CTR-RAXR study

INTRODUCTION

Calcite is a highly reactive and ubiquitous mineral in the Earth's crust. Abundantly present in sedimentary and metamorphic rocks (e.g. limestone, marble), calcite is also the main constituent of many biogenic and thermogenic deposits (i.e. tufa, travertine). The presence of calcite in many natural systems is of great importance due to its rapid dissolution/precipitation kinetics (Fenter & Sturchio, 2004), ion adsorption/desorption processes at the mineral-water interface, and the ability of calcite to incorporate impurities in its crystalline lattice (e.g. contaminants, toxic elements; cfr. Elziga et al., 2002), becoming an important natural trap for geological sequestration of pollutants in the environment.

Several studies have investigated ion adsorption and incorporation in calcite crystals (Cheng et al., 1999; Catalano et al., 2008; Fenter et al, 2008; Fenter & Sturchio, 2012; Lee et al., 2016). Many were focused on trapping of heavy metals and metalloids because of their high toxicity and common occurrence in geochemical systems. Arsenic behavior in natural systems has been extensively studied focusing on transport and trapping in the environment, evaluating the role of calcite in toxic metal incorporation and removal (Di Benedetto et al., 2006; Costagliola et al., 2013; Winkel et al., 2013). Environmentally relevant quantities are reported in many sites, especially in South East Asia which is the region that is most severely affected by natural As contamination in groundwaters, but also in Europe: France, Turkey, Greece (Winkel et al., 2013) and in many sites of central Italy (Costagliola et al., 2008; Di Benedetto et al., 2011; Costagliola et al. 2010). In the last cited works, Arsenic was found incorporated in calcite of present and Holocene travertine deposits. Similar results have been obtained also by Roman-Ross et al., (2006), Sø et al., (2008), Alexandratos et al., (2007) in calcite crystals which were precipitated in controlled conditions. Substitution of Arsenite [AsO_3^{3-}] after [CO_3^{2-}] has been argued to involve a distortion of the calcite lattice (Roman-Ross et al., 2006). In particular, the pyramidal Arsenite group produces an expansion of the c axis of the lattice of about 0.57-0.76 Å resulting in increased c-axe length and unit cell volume (Cheng et al., 1999; Romàn-Ross et al., 2006).

A similar effect has also been observed in the case of Arsenate-carbonate replacement, but at the same time it has been observed that Arsenate preferentially enters calcite due to its chemical properties (Sø et al. 2008; Alexandratos et al., 2007; Yokoyama et al., 2012). Arsenate concentrations reaching 900 ppm have been detected in some natural calcites (Winkler et al. 2013) and similar results for synthetic calcite had been published previously by Yokoyama et al. (2012).

The extent of As and Hg incorporation, however, and their distribution within the calcite lattice/crystal, has not been systematically investigated. Additionally, As uptake by calcite seems to

be enhanced by the presence of smaller cations (e.g. Mg) in the octahedral site that could balance the bigger size of Arsenite or Arsenate with respect to carbonate in the calcite lattice, thus promoting As incorporation (US Patent: 8,227,378). This effect has not been systematically studied yet.

Complexation of Hg (often associated to As in low-T hydrothermal fluids), with organic compounds and its adsorption onto mineral surfaces has been widely investigated (Sarkar D. et al, 1999; Yang et al., 2007; Rimondi et al., 2012) but there is no systematic study reporting on Hg adsorption onto the calcite surface, notwithstanding the numerous consequences that this interaction could have on the environmental sciences. In fact, despite their different geochemical behaviour (natural Hg-carbonates are very rare), Ca2+ has a ionic radius of about 0.98 Å while Hg^{2+} of 1.1 Å (very similar to 1.13Å of Sr^{2+} which is a common substitute of Ca^{2+} in calcite) and is likely that, under alkaline conditions, Hg^{2+} is adsorbed onto the negatively charged calcite surfaces, as happens for clay minerals (Yu et al., 2008), and maybe take part in the calcite precipitation process (Zhang et al., 2004).

Surface sciences which employ synchrotron radiation techniques are widely diffused in environmental studies of metal trapping into minerals, allowing the characterization of the uptake processes. The power of such techniques is documented by scientific literature. In this work we propose to use specular X-ray reflectivity experiments (*ex* and *in situ* CTR and RAXR) to probe the calcite-solution interface to understand how As and Hg are adsorbed and/or incorporated by the mineral surface during riequilibration and growth of the calcite with As- or Hg-bearing solution.

METHODS AND EXPERIMETAL

Atomic Force Microscopy (AFM)

Calcite dissolution and epitaxial growth was preliminary studied by means of Atomic Force Microscopy (AFM). In order to perform X-ray Reflectivity techniques it is essential to get atomically flat crystal surfaces, so it was necessary verify that bearing As and Hg calcite precipitates epitaxially onto (104) calcite surface. It is well known calcite's ability to dissolve and precipitate healing surface defects.

AFM measurements were carried out by means of Asylum Research MFP-3D-SA. In order to check that As and Hg uptake don't modify calcite surface, a (104) cleaved calcite crystal was kept in MFP Closed Fluid Cell which allow to study mineral surface topology in contact with a solution. A pumping system allows to inject a solution regulating the flux rate. The first part of experiment

consisted in the study of calcite dissolution by adding double distilled water to the cell. Dissolution process was followed for 1h imaging every 10 min. Subsequently a calcium carbonate saturated solution was injected in the fluid cell, following the process for 1h. The same samples were analyzed again in dry conditions after some days.

CaCO3 saturated solution was obtained by agitating calcite powder with double distilled water while in contact with the ambient atmosphere for two days and then filtered. At the end of the process it has been verified that saturation was reached and pH was about 8.3. From such stock solution As and Hg solutions were prepared. As arsenic sources were used sodium Arsenate dibasic heptahydrate $Na_2HAsO_4*7H_2O$ (Sigma Aldrich) for Arsenate, and arsenious acid (H_3AsO_3) in nitric acid solution 0.1N (Merk) for Arsenite. The final As concentration was fixed to 10 mM. In order to investigate the role of magnesium in As uptake each As^{III} and As^{V} batch was produced adding $MgCl_2$ to the solution in order to reach 10 mM concentration. Mercury was added to the calcium carbonate saturated solution as HgO in order to get a 0.1 mM solution.

X-Ray Reflectivity (XR) Measurements

Specular XR measurements were performed at Sector 13 (GeoSoilEnviroCARS) of the Advanced Photon Source (Argonne National Laboratory, Argonne IL). Crystal Truncation Rod (CTR) measurements were performed using a bending magnet radiation (13-BMC beamline) while Resonant Anomalous X-Ray Reflectivity (RAXR) measurements were performed at 13-IDC beamline using an ondulator source. In both cases the energy of radiation was 15.5kV, with a beam cross-section of 0.064x0.4 mm and a photon flux across it of about 10^9-10^{10} for bending magnet and over 10^{12} for ondulator radiation. Reflectivity signal was acquired by means of a CCD camera.

The calcite (104) surface was cleaved with a razor blade and quickly transferred (within seconds) to a calcite-saturated aqueous solution, in order to preserve the surface. About 1h before each experiment each crystal was transferred in an As or Hg enriched calcite saturated solution (as described above). In order to prevent Arsenite oxidation, such samples were treated, mounted and assembled in an oxygen-free glovebox and transferred in chamber continuously vented with nitrogen. Treated samples were mounted in a thin-film cell (Fenter et al., 2002) for X-ray Reflectivity characterization. The cell consist in an inert plastic (Teflon or PEEK) support where the calcite crystal is settled, covered with a thin polyimide film (Kapton™) which hold the solution. This cell geometry maintains small film of solution across the sample surface, and minimizes background intensity (e.g., due to X-ray scattering from the solution phase) by reducing the X-ray path-length through the solution (Fenter and Sturchio, 2004). During the course of the XR

measurements the sample was flushed frequently with the reaction solution (calcite saturated solution plus As or Hg): the solution was flowed into the cell expanding the membrane and thus exposing the sample to a fresh solution. This procedure was repeated two or three times for 10 minutes, allowing the solution to equilibrate with the sample. Such expedient was performed in order to prevent any modification of the mineral-water interface due to the low amount of solution and to prevent the formation of bubbles in the cell.

Samples were mounted on the goniometer head of a six circles diffractometer, and sample surface aligned to be parallel to incident beam at ϑ=0°. CTR measurements were carried out using Bragg-Brentano diffraction geometry.

The measure signal in X-ray reflectivity, R(Q), is the fraction of the incident beam flux that is reflected into the detector as a function of momentum change, Q. Because of the finite crystal structure at the mineral surface, this condition results in rods of intensity in reciprocal space, oriented perpendicular to the surface and passing through the reciprocal lattice points of the surface, as shown in Fig. 1. These rods are known as diffraction rods, or crystal truncation rods (CTR). Intensity changes along Qz following a periodic function with maximum in Bragg conditions and minimum in anti-Bragg conditions, resembling zero. Such intensity is function of the Structure Factor of surface which consider the upper, unmodified, structure of the crystal, the upper, relaxed, layers of atoms, eventually adsorbed ions or molecules and the liquid at the interface. Thus CTR analysis yields detailed probe about the fine structure of the crystal surface and water/crystal interface, reconstructing the electron density profile across the surface.

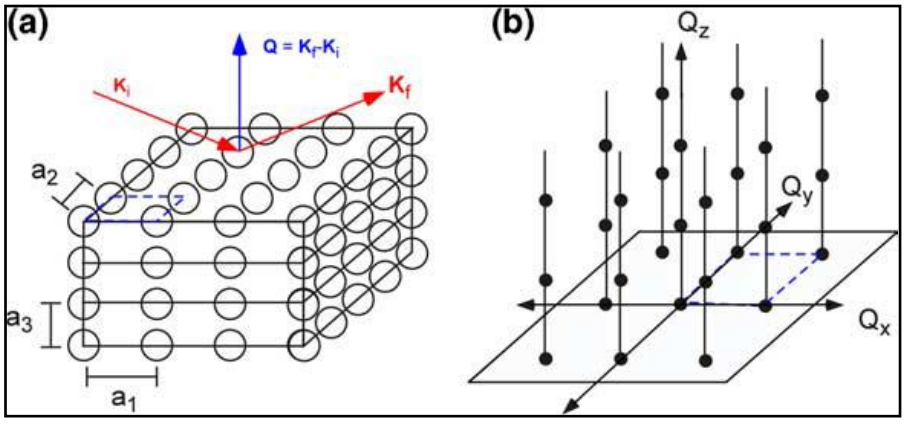

Fig. 1 – CTR theoretical scheme (from Fenter & Sturchio, 2004): a) A truncated crystal having surface lattice spacings a_1 and a_2 and layer spacing a_3. (b) The reciprocal-space structure for the truncated lattice.

Resonant anomalous X-ray reflectivity (RAXR) makes use of the 'anomalous' dispersion in the atomic scattering factor of an atom near its characteristic absorption edge. Briefly, the reflected intensity is measured as a function of energy near the absorption edge of the adsorbing cation at

fixed momentum transfer. Because the imaginary part of the resonant scattering factor, f''(E) is proportional to the X-ray absorption near edge structure (XANES) profile, this allows for the possibility of incorporating element-specific information into the X-ray scattering methods (Fenter et al., 2007; Fig. 2). In summary: XAS probes the energy dependence across a characteristic absorption edge, but it is not interface specific and does not provide unique information concerning the ion's location with respect to the surface; X-ray reflectivity (XR) CTR probes the q-dependent reflected intensity far from an absorption edge, thereby providing interface specificity but with little or no element specific information; RAXR brings together the structural sensitivity and interfacial specificity of X-ray reflectivity measurements with the element-specificity and spectroscopic sensitivity of XANES measurements leading to a much more complete understanding of the complex structural and chemical changes of many important interfacial processes (Park et al., 2005; Fenter et al., 2007; Lee et al., 2016). Experimentally, RAXR spectra are acquired across the As K-edge and Hg L-edge at different Q ($Å^{-1}$).

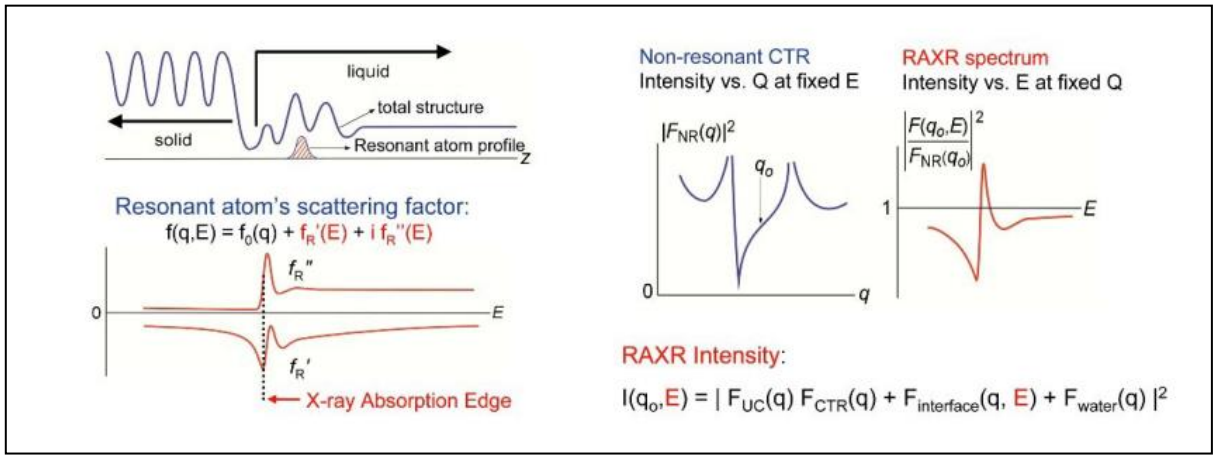

Fig. 2 – RAXR theoretical scheme in understanding surface structure and comparison with CTR (Fenter et al., 2007)

X-ray Absorption Spectroscopy (XAS)

In XAS measurements were used the As-bearing synthetic calcite samples used in Part 1, produced using Roman-Ross method (Roman-Ròss et al., 2006). Briefly, synthetic calcite was precipitated mixing 100 ml solution 0.5M Na_2CO_3, 1mM As (~75 mg/L), buffered at pH 8.9 with NaOH, with a solution 0.5M $CaCl_2$, added drop by drop for 1h, while stirring. Magnesian calcite was produced adding both 0.5M $CaCl_2$ and $MgCl_2$ solutions, maintaining Mg/Ca molar ratio <2%. Sodium Arsenate dibasic heptahydrate, $Na_2HAsO_4*7H_2O$ (Sigma Aldrich), and arsenious acid, H_3AsO_3, in nitric acid solution 0.1N (Merk) were used as Arsenic source for Arsenate (RR5, RR5Mg), and Arsenite (RR3), respectively. In order to avoid any Arsenite oxidation, the As^{III}-bearing calcite RR3

was precipitated in an oxygen-free chamber (O2 < 1ppm). The list of samples and their Arsenic concentration, obtained by means of ICP-OES (cfr. Part 1) is reported in Tab. 1. The same procedure was used to produce Hg-bearing calcite: 100 ml solution 0.5M Na_2CO_3, 0.1 mM Hg, buffered at pH 8.9 with NaOH, with a solution 0.5M $CaCl_2$, added drop by drop for 1h, while stirring. The precipitated powder was the washed three times in a calcite saturated solution and finally dried.

Both the As K-edge and Hg L-edge X-ray Absorption Spectroscopy (XAS) experiments were carried out on the at the GeoSoilEnviroCARS bending magnet beamline 13-BM-D were performed at 13-BMD beamline at the Advanced Photon Source (APS), Argonne National Laboratory (ANL), Argonne IL. The As K -edge XANES spectra were collected in fluorescence mode from -150 to 640 eV with 5 eV steps before the main edge (11871.5 eV for As^V; 11868 eV for As^{III}), and across the main edge (from -15 eV to 25 eV) with 0.25 eV steps, controlled with a Si(111) monochromator. The Hg L-edge spectra were collected in the same way at the L_{abII} (12285 eV) absorption edge.

Synthetic calcite samples were held between polyimide film tape (Kapton™) in punched plexiglass holders (as described above in Part 1), mounted in the X-ray beam at a 45° angle. X-ray fluorescence was recorded using a 19 element Ge solid-state array multi-element detector and the incident beam intensity (I_0) was recorded using a standard ionization detector. Energy calibration was performed using specific standard samples: Arsenic Oxide (As_2O_5), scorodite ($Fe^{3+}AsO_4 \cdot 2H_2O$) and schneiderhöhnite ($Fe^{2+}Fe^{3+}{}_3[As_5O_{13}]$), Arsenious Oxide ($As_2O_3$), Calcium Arsenate ($Ca_3(AsO_4)_2$) and Sodium Arsenate ($Na_2HAsO_4 \cdot 7H_2O$) for As^{III} and As^V K-edge and Mercury Oxide (HgO) for Hg L-edge. XAS scans were then merged and averaged to increase the intensity to noise ratio. Data DT correction and analysis was performed with Athena XAS data processing software, Demeter Pack (Ravel & Newville, 2005).

Tab 1. List of synthetic As-bearing calcite samples for XAS analysis

Sample	description	As in calcite (mg/kg)	As solution (mg/L)	Kd (L/kg) $[As]_{CAL}/[As]_{LIQ}$
RR5	Synthetic calcite	169	74.9	2.2
RR5Mg2	Synthetic calcite, Mg 2%	419	74.9	5.6
RR3	Synthetic calcite	2.3	74.9	0.03

RESULTS

Arsenic

AFM experiments of dissolution and epitaxial growth of calcite demonstrate how calcite(104) surface is extremely dynamic and reactive. In Fig. 3 are reported images of calcite dissolution: after

few minutes of interaction with double distilled water, some pits appear on the surface and their size increase as time passes. It is clear from Fig. 3 that pits sometimes follow calcite lattice, creating rhombohedral pits which follow the orientation of crystallographic axes, accordingly to the results reported by Teng et al. (2002).

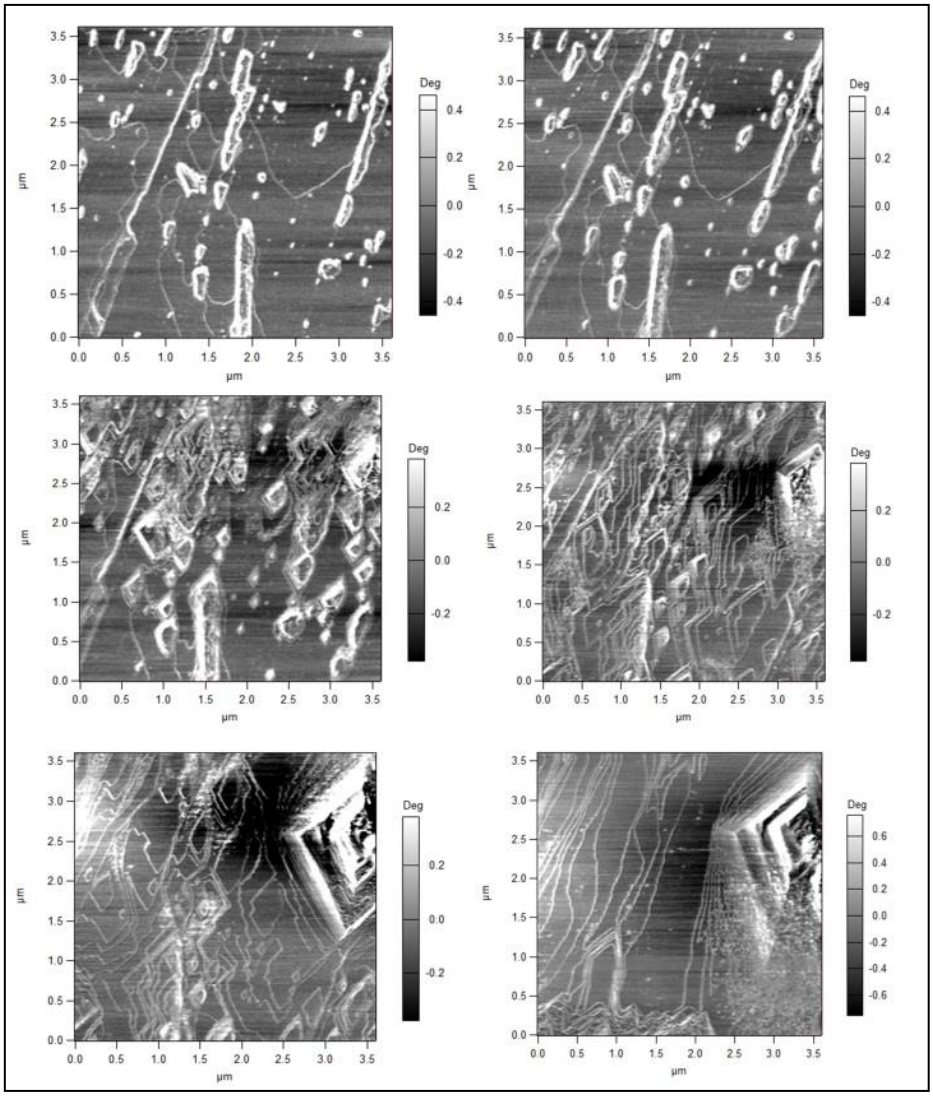

Fig. 3 – *In situ* AFM images of the dissolved (104) surface of calcite after injection of double distilled water. Pictures are taken every ten minutes for 1 hour.

Similarly surface epitaxial growth is as much fast: in Fig. 4 it is reported a complete 1h kinetic growth of calcite (104) surface following the dissolution process. In this case it is clear that all the pits made by the unsaturated water are quickly recovered by the calcite-saturated solution which creates a new flat surface precipitating layer by layer new epitaxial calcite. Such conditions are fundamental in order to perform XR measurements which require smooth and 'atomically flat' surfaces. The other interesting result arise from the observation that the presence of Arsenite or Arsenate (and eventually Mg), don't interfere with calcite growth and don't leave any particular feature on the new surface during real-time observations. On the contrary observations on Arsenate-

bearing dried samples revealed some particular features (as reported in Fig. 5.): these consist in swallowtail shaped pits orthogonally aligned to a-axis, on the c-glide (cfr. Paquette & Reeder, 1995) and concentrated on one side of calcite (104) surface. Finally, dried Arsenic-enriched calcite samples for XR measurements were characterized by means of XRF in order to verify that Arsenic actually attach calcite (104) surface. From Fig. 6 it is clear that Arsenate-bearing sample has a higher concentration of Arsenic with respect to Arsenite one, in agreement with XAS results on synthetic calcite samples.

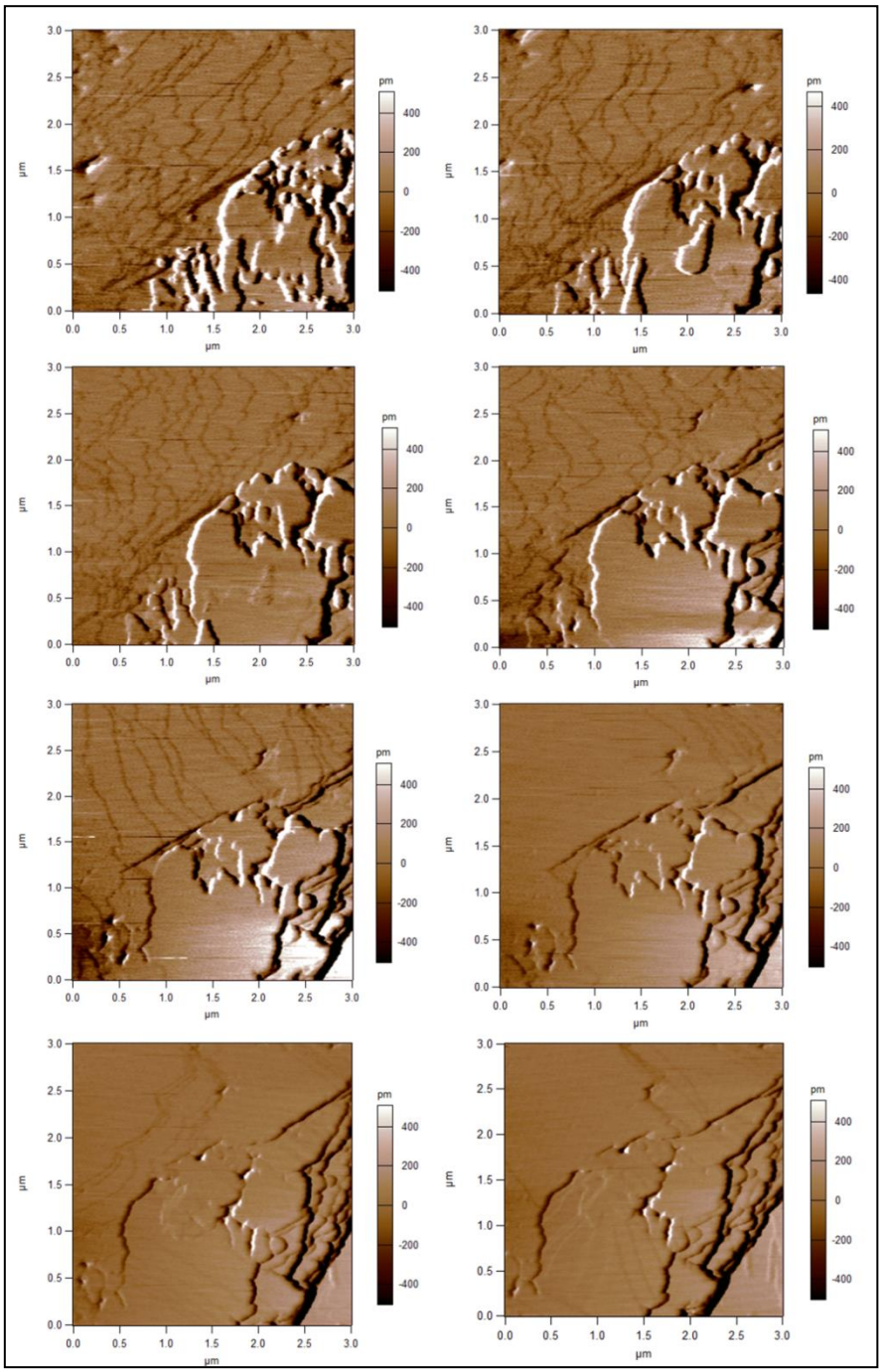

Fig . 4 – *In situ* AFM images of "reconstructed" calcite (104) surface after injection of calcite saturated solution, enriched with 0.1mM Arsenate. Pictures are taken every ten minutes for 1h and 20 min.

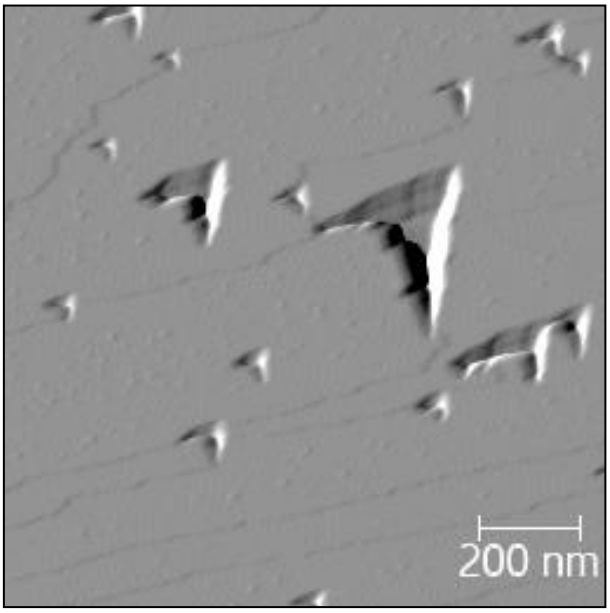

Fig. 5 – Ex situ AFM image of calcite (104) surface grown in 0.1 mM Arsenate solution.

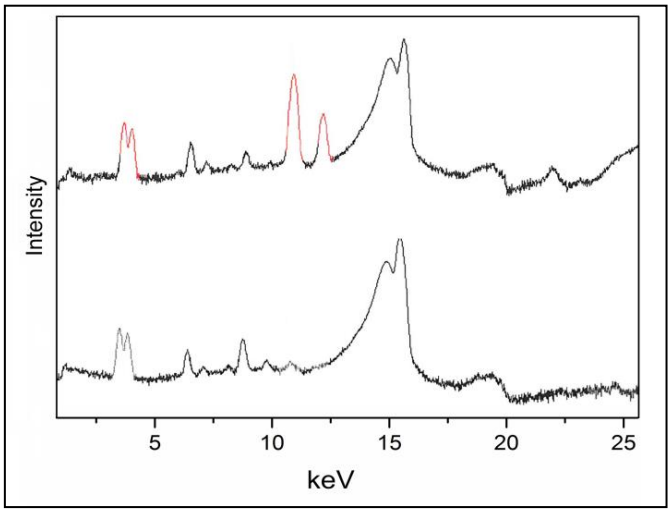

Fig. 6 – XRF spectra of calcite (104) surface treated with 0.1 mM Arsenate and Arsenite solution

Our CTR data (Fig. 7) exhibit the same qualitative features reported in literature (Fenter & Sturchio, 2004): large enhancements of the reflectivity are observed near Bragg reflections (observed at momentum transfer values of Q = n(2p/c) = 2.07, 4.14 and 6.21 $Å^{-1}$ where n is an integer). The reflectivity follows a characteristic U shaped curve between Bragg peaks as normally associated with the CTR shape (Fenter, 2002). The data are measured to the fourth Bragg peak (Q_{max} > 8 $Å^{-1}$) with a dataset of over 200 separately measured data points measured from Q = 0.41 to 8.1 $Å^{-1}$, of which 139 are distinct structure factors. The data also show a distinct modulation near the anti-Bragg conditions: near Q = 3.105 $Å^{-1}$ where there is a downward 'step' in reflectivity, and near Q = 5.176 $Å^{-1}$, where the reflectivity exhibits a weak and broad, but distinct, peak. Measurements on freshly cleaved calcite stored in calcite saturated solution compared with epitaxially grown ones didn't show any particular change in CTR spectra (Fig. 7)

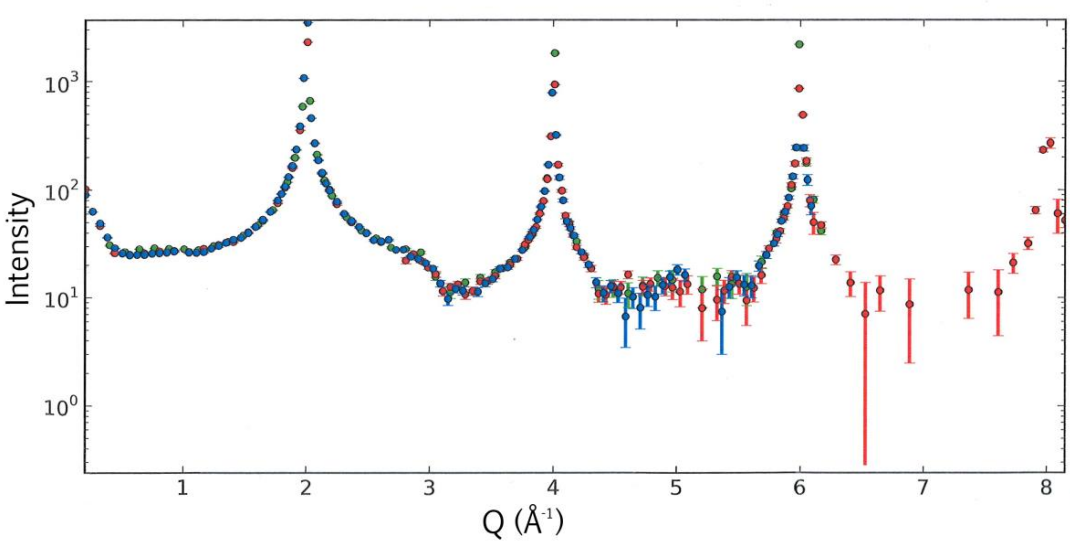

Fig. 7 – CTR pattern of three different calcite crystals: fresh cleaved calcite (red) and calcite after dissolution and epitaxial grown (green and blue)

For the subsequent measurements on As bearing calcites we decided to reduce the range of acquisition to the third order of Bragg peaks (Q = 6.3 Å^{-1}). As shown in Fig. 8, calcite grown in an Arsenate enriched medium has a different CTR pattern with respect to calcite, suggesting a different surface structure. In particular it is evidend a loss of intensity in the reflected signal in the first midzone and some features arise in the second one. RAXR measurements exhibit a weak but distinct modulation of the signal at the energy of the Arsenic, suggesting an ordered distribution of Arsenate in calcite structure. On the contrary Arsenite bearing calcite don't exhibit any difference in the CTR pattern nor in the RAXR, suggesting low modifications in calcite surface lattice, probably due to the very low amount of As incorporated during calcite growth.

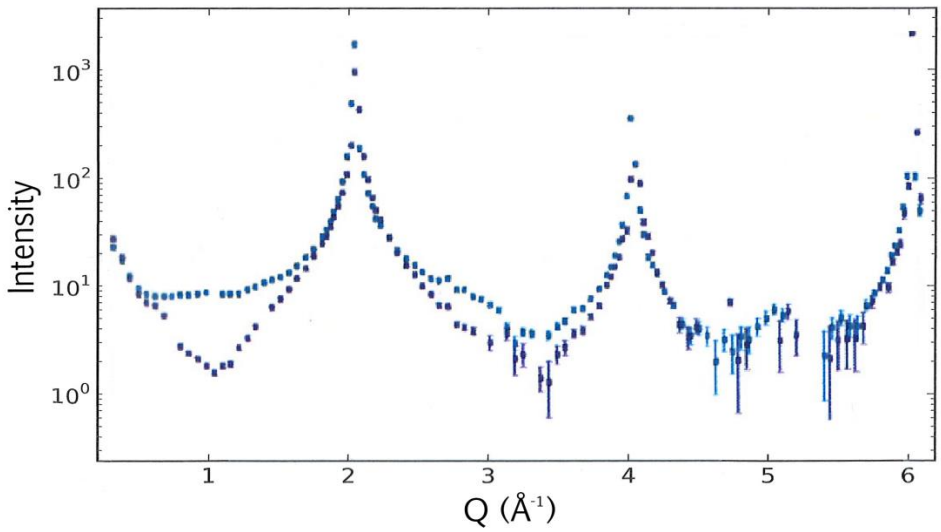

Fig. 8a – CTR pattern of calcite (104) treated with 0.1mM Arsenate solution (violet) compared with calcite (blue).

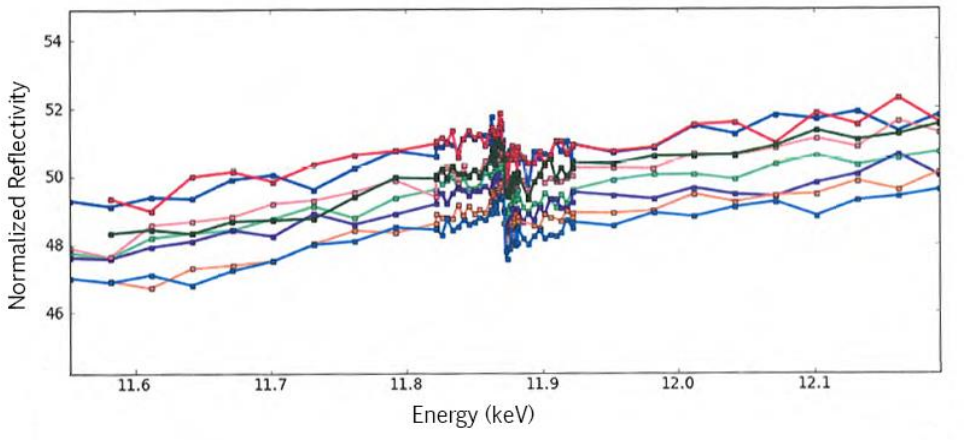

Fig. 8b – RAXR spectrum of calcite (104) treated with 0.1mM Arsenate solution measured across the As absorption K-edge, at different Q ($Å^{-1}$).

XAS patterns acquired on Arsenate-bearing calcite clearly show the absorption edge of As^{V} and there are no difference between the Mg-free and Mg-bearing calcite (Fig. 9a), while RR3 spectrum (merged from 12 measurements) exhibit both As^{III} (weaker) and As^{V} absorption edges. In both RR5 and RR5Mg the spectral area close to the As absorption K-edge (11871.5 eV) has only a broad band at about +15eV. Converting XAS data in k-space, we observed for all the three samples a single frequency oscillation without any particular feature (Fig. 9c). Finally, from XAS spectra converted in R-space (Fig. 9c) it is clear that both the Arsenate-bearing samples have a distinct first coordination shell, corresponding to As-O bonding of Arsenate, but there are no other peaks in the region 2-6 Å. As regards the Arsenite bearing calcite (RR3), the XAS spectrum exhibit both the As^{III} and As^{V} K-edges, despite all the experiments were carried out in glovebox with a controlled O_2 pressure (<10ppm) and sample transfer and measurements were performed using a chamber vented with nitrogen.

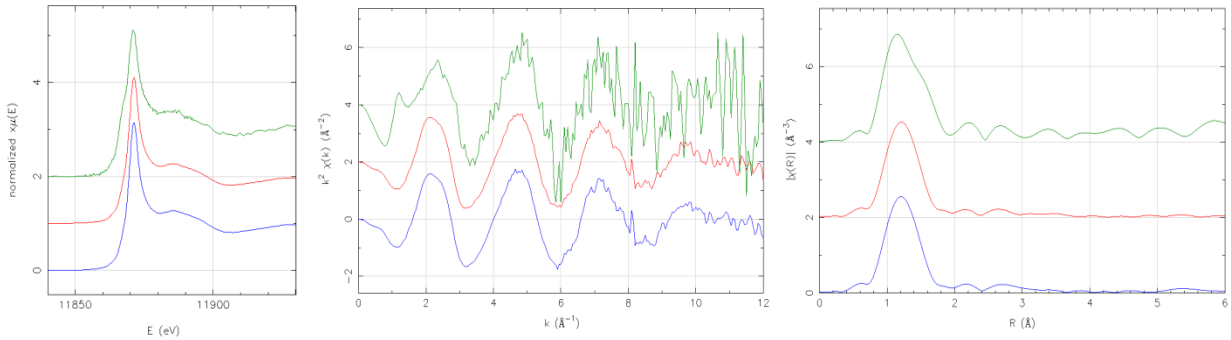

Fig. 9 – Normalized XAS spectra of RR3 (green), RR5 (red) and RR5Mg (blue), in E-space (a), k-space (b) and R-space (c).

From R-space converted XAS data it is clear the presence of a double first coordination atoms shell corresponding to Arsenite and Arsenate, but even in this case there are no evidence of second coordination shell. Another interesting result arises from the time-resolved XAS measurements on Arsenite bearing calcite: in fact, as shown in Fig. 10, after each scan the Arsenite/Arsenate ratio decreases from the initial 1.2 to the final 0.3.

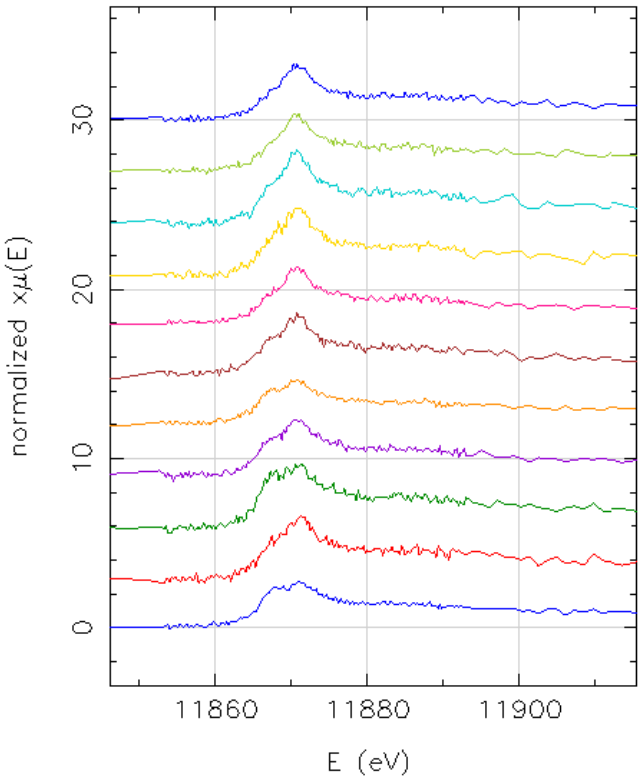

Fig. 10 – XAS spectra of RR3 in time from the first measurements (bottom) to the last (top).

Mercury

AFM measurements on Hg-bearing calcite didn't show any difference with respect of As during the dissolution/growth experiment. In fact it was observed the same process of roughen during the double-distilled water treatment and subsequent surface healing and smoothing when the calcite saturated solution was injected in the liquid cell. At the end of this experiment the sample was washed in calcite saturated solution, dried and analyzed after 4 hours and 2 days since the epitaxial growth experiment. As shown in Fig. 11a and 11b, the sample surface was radically changed: after 4 hours some particles appeared onto the surface (bright spots) and after 2 days the surface was completely covered by a bubble-shaped cover. XRD measurements confirmed the presence of Hg onto calcite surface.

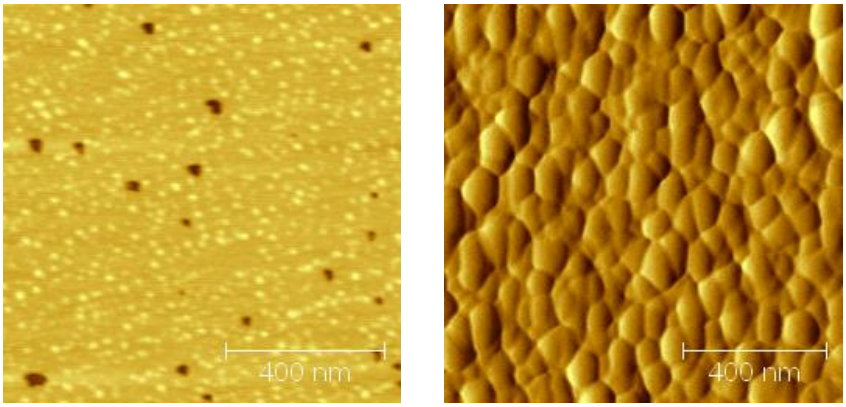

Fig. 11 – *Ex situ* AFM images of dried calcite (104) surface after 1h treatment with calcite saturated solution, 0.1mM Hg. Pictures are taken every 2 hours (left) and 2 days (right), respectively.

CTR pattern on calcite treated 1hr with Hg solution shows the same features of the standard calcite patterns while RAXR signal is absolutely absent (Fig 12a). Subsequent CTR measurements on dried calcite exhibit a huge variation of CTR pattern in the first and second mid-zones, whit a distinct change of intensity around 0.8 and 3 $Å^{-1}$ (Fig. 12b).

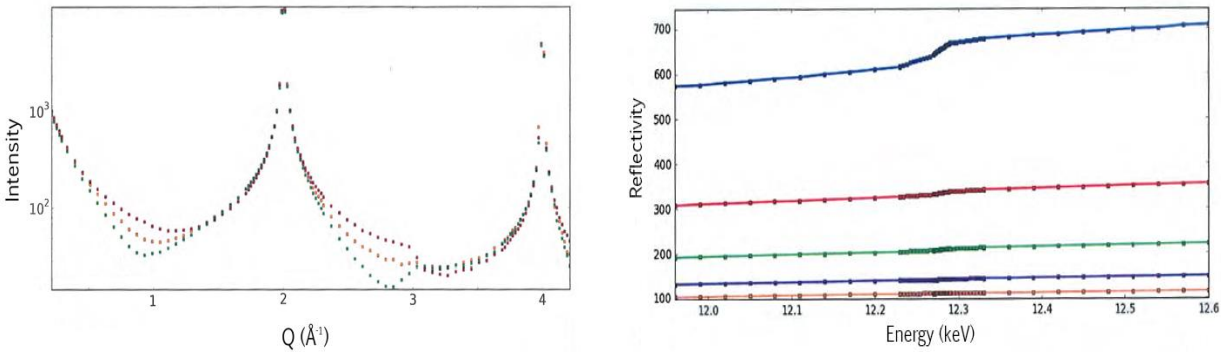

Fig.12 – Hg treated calcite after 1h treatment (orange), and dried after 4 hours and two days (red), CTR pattern (a). RAXR meaurements on 1h Hg-treated sample at different Q (b).

Finally, Hg-bearing synthetic calcite XAS spectra measured at the L-absorption edge (Fig 13a) exhibit a three step pattern, highlighted in Fig 13b where are shown the derivative spectra. The first edge (12282.5 keV) correspond to the XAS pattern of HgO, accordingly to literature data (Serrano et al., 2012; Bernaus et al., 2005), the second (and 12295.4 keV) partially overlap the HgO absorption edge, while the third (12309.3 keV), the more distinct one, seems to be characteristic of Hg in calcite. From transformed R-space spectra it is clear how HgO has a single first order peak, corresponding to Hg-O bond (about 2.1 Å). Synthetic calcite with Hg exhibit a double first order peak, one corresponding to Hg-O length of HgO and a second shell at about 2.3-2.4 Å, corresponding to Hg trapped in calcite. In the range 2-6 Å HgO has non particular features,

suggesting low crystallinity of the standard, while Hg-bearing calcite has a weak but distinct peak at about 3.3 Å.

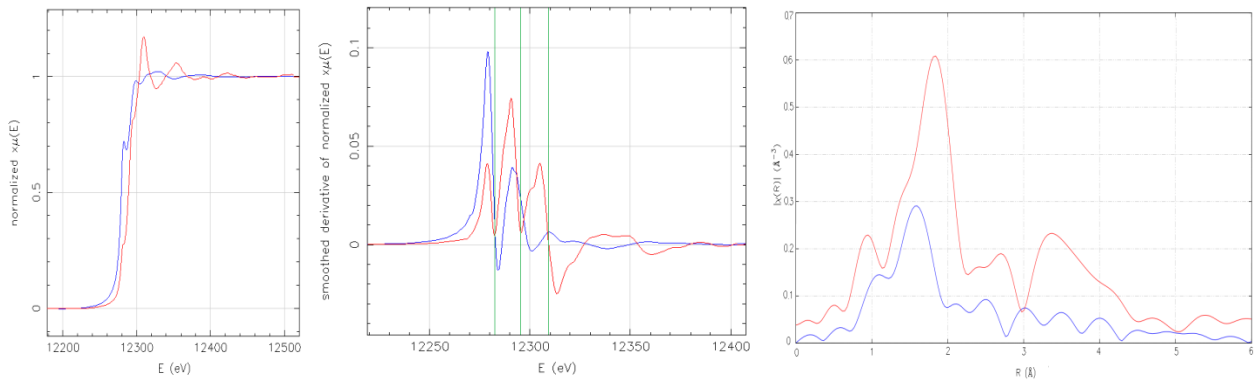

Fig. 13 – XAS spectrum of HgO (blue) and Hg-bearing calcite (red) in E-space (a), as derivative (b; the green lines correspond to the absorption edges in Hg-bearing calcite) and converted in R-space (c).

DISCUSSION

AFM imaging on calcite (104) surface confirm how calcite surface can easily heal after dissolution. Such results are not surprising, and confirm that the fast kinetic in dissolution and precipitation is well suitable for metal trapping. In particular many authors (Cheng et al, 1999 ; Alexandratos et al., 2007) debated about the residual charge on calcite (104) surface which permit to charged ions and oxyanions to attach the surfaces and be trapped during calcite precipitation.

Our results on As-bearing calcite, basically confirm such picture, adding some new insights. First of all, from dissolution/precipitation experiments on calcite (104) surface it is clear that calcite easily heal after dissolution growing new epitaxial calcite. The result is a new smooth surface reconstructed from the calcite saturated solution. Such procedure allows the use of x-ray reflectivity techniques in order to investigate the uptake of Arsenic and Hg into calcite lattice. Secondly, during the in situ experiments there were no evidences of precipitation of other phases more than calcite, in agreement with As-bearing synthetic calcite produced with Roman-Ròss method (RR5, RR5Mg and RR3). The only marker we observed in epitaxially grown Arsenate-bearing calcite are the swallowtail shaped pits shown in Fig.5, aligned on the minor diagonal of rhombohedral (104) surface (c-glide as reported in literature; cfr. Paquette & Reeder, 1995 and Alexandratos et al., 2007). Such markers have never been reported before in literature, and are an element of novelty. In order to explain how they built up, the only clue we have it is their location onto the (104) surface. In fact they are all aligned in the same direction and mainly concentrated on one side of the calcite crystal. Alexandratos et al. (2007) reported how Arsenate preferentially absorbs and concentrates in

some vicinal zones on one side of calcite (104) crystal face. They found an explanation to this effect by considering the difference in surface atomic structure on one side of calcite crystals, as previously debated by Paquette & Reeder (1995), differentiating in growth steps + and –. Briefly, both the ion metals which substitute Calcium and structurally incompatible anions which replace carbonate could prefer + or – steps for adsorption and subsequent incorporation: Arsenate oxyanions prefer the – growth steps and it concentrates on that side. As a consequence of such phenomenon there are some areas on the surface with higher As content with respect to others. From literature (Roman-Ross et al., 2006) and from our results reported in Part 1, it is clear that As-bearing calcite has an elongated c-axe due to steric effect of pyramidal Arsenate and Arsenite with respect of planar carbonate. Such difference could produce a misfit in calcite growth between areas with different As concentrations which produces the pits seen only onto Arsenate-bearing calcite. On the contrary, no evidence of such pits emerged in Arsenite-bearing calcite, probably due to the low amount of As trapped in calcite during surface growth. Such result is confirmed by XRF data on epitaxially grown calcite (Fig. 6) and from chemical analysis of synthetic calcite (Tab. I). In particular, synthetic calcite allow us to estimate an enrichment factor of 4 order higher for Arsenate with respect to Arsenite, with a positive effect of Mg in As uptake. Such results are already debated in Part 1, but briefly we can argue that Arsenite uptake is much lower than Arsenate due to the almost neutral charge of arsenious acid in the common pH range for calcite precipitation (8-9), so its ability to adsorb onto calcite surface or link Ca^{2+} for co-precipitation is highly reduced with respect to Arsenate, which is almost totally dissociated in that pH range.

XAS data allow us to investigate the incorporation process in calcite. The diagnostic features are spectral area close to the As absorption K-edge and the second order oscillation in k-space converted spectra, as widely discussed in Part 1. In particular the spectral range 2.5-6 $Å^{-1}$ in k-space exhibit a single broad peak, typical of Arsenic absorbed onto calcite. Comparing our results (Fig. 9a-b) with those reported in literature (Winkel et al., 2013) and in Part 1, it is clear that that As uptake in synthetic calcite is mainly driven by oxyanion absorption onto surface, and subsequent trapping. Another outcome regards the Arsenic ordering in calcite structure: neither Arsenate, nor Arsenite, exhibit a second coordination shell (Fig. 9c). In fact in RR5 and RR5Mg R-space spectra it is evident the first coordination shell, corresponding to 1.69 Å of Arsenate As-O bond, while there are no peaks in the region 2-6 Å. Regarding RR3, the R-space spectrum exhibit a double peak corresponding to the different As-O bond length of Arsenate (1.69 Å) and Arsenite (1.81 Å). The absence of a second atomic coordination shell suggest that the uptake process just incorporate As without any ordering in calcite crystal lattice. Regarding Arsenate, these findings are coherent with those reported in Part 1 for Bullicame Travertines and form literature (Winkel et al., 2013).

Regarding Arsenite, on the other hand, we didn't found any ordering in calcite structure just like in biogenic calcite reported in Part 1. Such findings are in contrast with literature data (Cheng et al., 1999; Di Benedetto et al., 2006; Bardelli et al., 2011), suggesting that the Arsenite uptake process could influence the As trapping in calcite. Arsenate and Arsenite adsorption from supersaturated solution, just like the biogenic process, seems to trap Arsenic in calcite without any ordering in calcite crystalline lattice.

Finally, XAS analysis of Arsenite bearing synthetic calcite yield two interesting results. First, despite experiments were carried out in oxygen free environments, As trapped in calcite is both Arsenite and Arsenate (Fig. 9), suggesting that As^{5+}, if any, present in the solution it is preferentially trapped in calcite, in agreement with the results reported by Yokoyama et al. (2012). Second, time resolved XAS measurements exhibit a clear decrease of Arsenite/Arsenate ratio. At the beginning Arsenite was the prevalent form of Arsenic trapped, while at the end it was less than 1/3. Thi experiment demonstrates that, even if the measurements were performed in oxygen-free atmosphere, Arsenite easily oxidizes to Arsenate, probably catalyzed by the X-ray irradiation of the sample. Such result is not coherent with measurements made on biogenic calcite in Part 1 where we didn't observe any change in Arsenite/Arsenate ratio during the measurements, suggesting that in biogenic calcite Arsenite is trapped in a different, more stable, way with respect of synthetic RR3.

CTR and RAXR data acquired on epitaxially grown calcite allow us to further understand the Arsenic uptake process onto calcite. First of all CTR spectra acquired onto calcite grown with Arsenate show clear changes in the first and second midzones, suggesting changes in the surface structure. Such changes are due to Arsenic incorporation in calcite which modify calcite lattice to accommodate Arsenate oxyanion in carbonate site. Such changes are not seen in Arsenite treated samples, probably because of the low amount of Arsenic which precipitates with the new calcite. Finally RAXR data from Arsenate treated samples exhibit a weak but distinct modulation of signal, indicating that there is an Arsenate ordering in calcite lattice during the uptake process.

Such results are in contrast with XAS data from synthetic calcite precipitated from supersaturated solution (Roman-Ròss et al. 2006 method), suggesting a different process of Arsenic uptake. Of course, it seems clear that the uptake process involved in epitaxial growth of calcite allow Arsenate to order inside the crystal lattice. It is likely that the lower kinetic of calcite growth and the geometry of the surface could allow the ordering.

Regarding Mercury, our data suggest that uptake process takes place in some way, but it is not straightforward in the interpretation. First of all AFM measurements on epitaxially grown calcite with enriched Hg solution suggest calcite growth process is the same, but that after the Mercury is trapped there's a sort of requilibration of Hg which produce particle nucleation on the surface and

subsequent modification of surface morphology. In literature there are few data about the effect of Mercury on calcite surface structure. Actually, the only reference is from Godelitsas et al., 2003, where they analyzed the interaction between Hg(II)-solution with (104) calcite surface. Despite their experiments were designed quite different from ours (namely, different Hg source and concentration, and chemical composition of interacting solution), they reported about formation of small nanometric Mercury crystal and spheres onto calcite surface after interaction. It seems to be coherent with our findings, in fact we observed particle nucleation and growth onto calcite surface, suggesting that Mercury, besides the uptake in calcite, precipitates its own phases. Differently from the cited work, we didn't observe any particular marker (e.g. pits) on the calcite surface during AFM in situ measurements.

XAS data revealed that Mercury trapped in calcite is present, likely, both as oxide and in another form. The presence of HgO could be argued by the XAS spectrum (Fig. 13a) where it is clear that a part of spectrum well resemble the Hg absorption L_{abII}-edge of HgO. Moreover, converting Hg-bearing calcite XAS spectrum in R-space, it exhibits a double first-order coordination shell: the first Hg-O bond is about 2.1 Å and it commensurate with Hg-O length in Mercury(II) Oxide, while the second, more intense, one has a longer Hg-O of about 2.3-2.4Å. Such value is very close to the Ca-O bond length (Paquette & Reeder, 1990), and could suggest a substitution Hg-Ca in calcite crystal lattice, due to the similar ionic radius of Ca^{2+} (0.98 Å) with Hg^{2+} (1.1 Å). Even if such explanation seems straightforward, RAXR data clearly suggest that Hg^{2+} doesn't order inside calcite crystal lattice substituting Ca^{2+}. In fact RAXR pattern doesn't show any modulation of intensity. On the contrary, aged Hg-treated calcite crystal exhibit CTR spectra with wide and clear change of intensity in the first two midzones with crystal aging (4 hours and 2 days). Such variations are not the typical CTR modulation of intensity due to surface adsorption/precipitation of ions, but probably are due to extensive surface relaxation effects.

CONCLUSIONS

Our results on Arsenic and Mercury uptake in calcite highlight new and interesting critical point in understanding the process, although the work is not yet completed and the state of the art still in progress. Regarding Arsenic, our findings in part confirmed the picture which arise from literature: basically it is confirmed that Arsenate is preferentially trapped in calcite with respect to Arsenite, because of the chemical properties of the two species that are widely debated in literature. Anyway, in opposite to literature records, our data suggest that in particular conditions Arsenate could precipitate in calcite, likely substituting carbonate and ordering inside the crystal lattice. Further and

more deepen analysis on CTR and RAXR data will provide more details about the uptake process and Arsenic adsorption and incorporation in calcite, with respect to the merely qualitative approach we adopted.

Regarding Mercury, our work could be considered pioneering in understanding the uptake process in calcite, since in literature there are no studies about it. Our main findings regard the ability of calcite to trap in Mercury, even if it seems quite complicated to explain the uptake process in all its parts. In particular we have many clues that Hg-bearing calcite is not stable with aging: AFM imaging and CTR data suggest a huge transformation of calcite (104) surface, suggesting that calcite is not stable when a critical amount of Mercury sink in its crystal lattice.

References

Alexandratos V.G., E.J. Elziga, R.J. Reeder (2007) Arsenate uptake by calcite: Macroscopic and spectroscopic characterization of adsorption and incorporation mechanisms. *Geochimica et Cosmochimica Acta* 71: 4172–4187

Angelone M., C. Cremisini, V. Piscopo, M. Proposito, Fabio Spaziani (2009) Influence of hydrostratigraphy and structural setting on the arsenic occurrence in groundwater of the Cimino-Vico volcanic area (central Italy). *Hydrogeology Journal* 17: 901–914

Bardelli F., M. Benvenuti, P. Costagliola, F. Di Benedetto, P. Lattanzi, C. Meneghini, M. Romanelli, L. Valenzano (2011) Arsenic uptake by natural calcite: An XAS study. *Geochimica et Cosmochimica Acta* 75: 3011–3023

Bernaus A., X. Gaona, M. Valiente (2005) Characterisation of Almadén Mercury mine environment by XAS Techniques Journal of Environmental Monitoring 7: 771-777

Catalano J.G., C. Park, P. Fenter, Z. Zhang (2008) Simultaneous inner- and outer-sphere Arsenate adsorption on corundum and hematite *Geochimica et Cosmochimica Acta* 72(8): 1986-2004

Cheng L., P. Fenter, N.C. Sturchio, Z. Zhong, M.J. Bedzyk (1999) X-ray standing wave study of Arsenite incorporation at the calcite surface *Geochimica et Cosmochimica Acta* 63(19/20): 3153–3157

Costagliola P., M. Benvenuti, L. Chiarantini, S. Bianchi, F. Di Benedetto, M. Paolieri, L. Rossato (2008) Impact of ancient metal smelting on arsenic pollution in the Pecora River Valley, Southern Tuscany, Italy *Applied Geochemistry* 23: 1241–1259

Costagliola P., M.M. Benvenuti, M.G. Benvenuti, F. Di Benedetto, P. Lattanzi (2010) Quaternary sediment geochemistry as a proxy for toxic element source: A case study of arsenic in the Pecora Valley (southern Tuscany, Italy) *Chemical Geology* 270(1–4): 80-89

Di Benedetto F., P. Costagliola, M. Benvenuti, P. Lattanzi, M. Romanelli, G. Tanelli (2006) Arsenic incorporation in natural calcite lattice: Evidence from electron spin echo spectroscopy. *Earth and Planetary Science Letters* 246: 458 – 465

Di Benedetto F., G. Montegrossi , A. Minissale, L.A. Pardi, M. Romanelli, F. Tassi, A. Delgado Huertas, E.M. Pampin, O. Vaselli, D. Borrini (2011) Biotic and inorganic control on travertine deposition at Bullicame 3 spring (Viterbo, Italy): A multidisciplinary approach. *Geochimica et Cosmochimica Acta* 75: 4441–4455

Elziga E.J. and R.J. Reeder (2002) X-ray absorption spectroscopy study of Cu^{2+} and Zn^{2+} adsorption complexes at the calcite surface: Implications for site-specific metal incorporation preferences during calcite crystal growth. *Geochimica et Cosmochimica Acta* 66(22): 3943–3954

Fenter P., P. Geissebühler, E. DiMasi, G. Srajer, L.B. Sorensen, N. C. Sturchio (1999) Surface speciation of calcite observed in situ by high-resolution X-ray reflectivity. *Geochimica et Cosmochimica Acta* 64(7): 1221–1228

Fenter P. (2002) X-ray reflectivity as a probe of mineral–fluid interfaces: a user guide. *Reviews in Mineralogy and Geochemistry* 49, 149–220.

Fenter P., N.C. Sturchio (2004) Mineral–water interfacial structures revealed by synchrotron X-ray scattering. *Progress in Surface Science* 77: 171–258

Fenter P., C. Park, K.L. Nagyb, N.C. Sturchio (2007) Resonant anomalous X-ray reflectivity as a probe of ion adsorption at solid–liquid interfaces *Thin Solid Films* 515: 5654-5659

Fenter P., N.C. Sturchio (2012) Calcite (104)–water interface structure, revisited. *Geochimica et Cosmochimica Acta* 97 (2012) 58–69

Godelitsas A., J.M. Astilleros, K.R. Hallam, J. Lons, A. Putnis (2003) Microscopic and spectroscopic investigation of the calcite surface interacted with Hg(II) in aqueous solutions *Mineralogical Magazine* 67(6): 1193–1204

Lee S.S., F. Heberling, N.C. Sturchio, P.J. Eng, P. Fenter (2016) Surface Charge of the Calcite (104) Terrace Measured by Rb+ Adsorption in Aqueous Solutions Using Resonant Anomalous X-ray Reflectivity *Journal of Physical Chemistry* 120: 15216−15223

Park C., Fenter P. A., Sturchio N. C., and Regalbuto J. R. (2005) Probing outer-sphere adsorption of aqueous metal complexes at the oxide-water interface with resonant anomalous X-ray reflectivity. *Physical Review Letters* 94(7): 96-104

Paquette J., R.J. Reeder (1990) Single-crystal X-ray structure refinements of two biogenic magnesian calcite crystals. *American Mineralogist* 75: 1151-1158

Paquette J., RJ Reeder (1995) Relationship between surface structure, growth mechanism, and trace element incorporation in calcite *Geochimica et Cosmochimica Acta* 59(4): 735-749

Ravel B., M. Newville (2005) ATHENA, ARTEMIS, HEPHAESTUS: data analysis for X-ray absorption spectroscopy using IFEFFIT. *Journal of Synchrotron Radiation* 12: 537–541

Rimondi V., J.E. Gray, P. Costagliola, O. Vaselli, P. Lattanzi (2012) Concentration, distribution, and translocation of mercury and methylmercury in mine-waste, sediment, soil, water, and fish collected near the Abbadia San Salvatore mercury mine, Monte Amiata district, Italy *Science of the Total Environment* 414: 318–327

Román-Ross G., G.J. Cuello, X. Turrillas, A. Fernández-Martínez, L. Charlet (2006) Arsenite sorption and co-precipitation with calcite. *Chemical Geology* 233: 328 – 336

Sarkar D., M.E. Essington, K.C. Misra (2000) Adsorption of Mercury(II) by Variable Charge Surfaces of Quartz and Gibbsite *Soil Sciences Society of America Journal* 64: 1968–1975

Serrano S., D. Vlassopoulos, B. Bessinger, P.A. O'Day (2012) Immobilization of Hg(II) by Co-precipitation in Sulfate-Cement Systems *Environmental Science and Technology* 46: 6767−6775

Sø H.U., D. Postma, R. Jakobsen, F. Larsen (2008) Sorption and desorption of Arsenate and Arsenite on calcite. *Geochimica et Cosmochimica Acta* 72: 5871–5884

Winkel L.H.E., B. Casentini, F. Bardelli, A. Voegelin, N.P. Nikolaidis, L. Charlet (2013) Speciation of arsenic in Greek travertines: Co-precipitation of Arsenate with calcite. *Geochimica et Cosmochimica Acta* 106: 99–110

Yang Y., L. Liang, D. Wang(2008) Effect of dissolved organic matter on adsorption and desorption of mercury by soils *Journal of Environmental Sciences* 20(2008) 1097–1102

Yokoyama Y., K. Tanaka, Y. Takahashi (2012) Differences in the immobilization of Arsenite and Arsenate by calcite. *Geochimica et Cosmochimica Acta* 91: 202–219

Yu X., L. Zhu, B. Guo, S. He (2008) Adsorption of mercury on laterite from Guizhou Province, China *Journal of Environmental Sciences* 20: 1328–1334

SUMMARY AND CONCLUSIONS

Arsenic uptake in calcite has been investigated, concentrating both on the bio-mediate and the chemical process. The bacterial precipitation of calcite is a well known process but the main element of novelty is represented by its use in sinking Arsenic in a stable and environmentally important phase. In order to investigate the uptake process a comparison with natural travertines was performed and results yield new insights in the understanding of Arsenic bio-mediated uptake other than new perspectives in its application to environmental threats.

An interesting outcome of this research regards the ability of bacteria to sink Arsenite in calcite. In fact, form literature works (cfr. Yokoyama et al., 2012) it was clear that only Arsenate is suitable to sink in calcite in the common environmental pH and chemical conditions. More in detail, it is confirmed that bacteria are able to act a direct control onto Arsenic cycle and by mediating mineral precipitation. In this case *B. licheniformis* showed the ability to reduce Arsenate to Arsenite performing a detoxification process by means of cytoplasmic reaction chain which involve the Arsenate reductase proteins ArsC and ArsB and subsequent Arsenite excretion by means of specific transport proteins (Silver & Phung, 2005) and finally the ability to sink Arsenite into microbially precipitated calcite. Such processes seems to be strongly dependent on the environmental conditions in which bacteria live: in fact the two batch of samples produced in liquid and solid culture medium exhibit radically different chemical and mineralogical properties. Despite the initial Arsenic concentration and speciation in the two media was the same, solid-cultured bacteria precipitated calcite with both Arsenate and Arsenite species, and made up by sole calcite while the liquid-cultured ones are made by calcite and vaterite, with the sole Arsenate, suggesting that environmental conditions highly influence the uptake process.

Another interesting outcome regards the amount of Arsenic that bacterial calcite are able to sink: solid-cultured samples have, in fact, As concentrations lower than 50 ppm, with an enrichment factor (measured as Kd = [As]solid/[As]liquid) quite low. On the contrary liquid-cultured calcites reached As concentrations higher than 1000 ppm, with Kd commensurate with those of Bullicame Hot Springs travertines. Similarities between liquid-cultured bacterial calcite and natural travertines arise from XAS data regarding the uptake process, suggesting that such conditions well resemble the natural process of As sink. As a consequence, we think that the use of bacteria to induce calcite precipitation in Arsenic polluted areas and springs could be an efficient process of bioremediation,

and it could be considered the idea to patent the bacterial treatment of As-polluted waters by means of *B. licheniformis*.

Another interesting outcome arises from the effect of Magnesium during calcite precipitation. In detail, our results suggest that the presence of a slight amount of Mg (about 1%) positively affect Arsenic uptake in calcite. Despite such effect was already observed an patented (), no explanation was previously reported. Our XRD data suggest that Arsenic uptake in calcite produces as a direct effect the elongation of c-axe of calcite cell, as predicted and debated by some authors which attribute such change to the steric effect of pyramidal Arsenite or tetrahedral Arsenate with respect to planar geometry of carbonate group. On the opposite Mg^{2+} has minor atomic radius with respect to Ca^{2+} cation, showing an opposite effect (Paquette & Reeder, 1990), which could compensate the Arsenic one, thus allowing to better accommodate Arsenate and/or Arsenite into calcite crystalline lattice. This result is very interesting and could involve other trace elements which positively or negatively affect Arsenic uptake in calcite.

Regarding the chemical process of Arsenic uptake, the novelty of this work regards the analytical approach which has never tried before. In fact, all the previous studies used bulk techniques which reconstructed the whole uptake process, while using X-ray Reflectivity techniques we decided to focus only on the mineral-water interface in order to probe how Arsenic attaches the surface, how it sinks and how it is accommodated in calcite during the epitaxial growth of (104) crystallographic surface. Our findings basically confirm that Arsenate is preferentially trapped in calcite with respect to Arsenite, because of the chemical properties of the two species that are widely debated in literature (Yokoyama et al., 2012). Anyway, new findings arise from merely qualitative analysis of our data: in fact in opposite with all previous works which report that there is no ordering of Arsenate in calcite, our RAXR data clearly indicate that superficial Arsenate which precipitate in calcite during (104) epitaxial growth is ordered, likely substituting carbonate. Further and more deepen analysis on CTR and RAXR data will provide more details about the uptake process and Arsenic adsorption and incorporation in calcite, with respect to the merely qualitative approach we adopted.

The same approach we used for Arsenic was used to study Mercury uptake in calcite. In literature there are no records about such process, so our work could be considered pioneering in understanding if Mercury could be trapped in calcite substituting Calcium. Our findings confirm that Mercury is trapped in calcite during its precipitation, but it seems quite complicated to explain how the process takes place. In particular we observed a distinct behavior depending on the precipitation process: in calcite precipitated by supersaturated solution XAS data seems to suggest that Hg^{2+} replace Ca^{2+} in calcite structure, but no evidences of such ordering form RAXR

measurements on epitaxially grown calcite(104). Finally, we have many clues that Hg-bearing calcite is not stable with aging: AFM imaging and CTR data suggest a huge transformation of calcite-104 surface, suggesting that calcite is not stable when a critical amount of Mercury sink in its crystal lattice.

References

Aredes S., B. Klein, M. Pawlik (2012) The removal of arsenic from water using natural iron oxide minerals. *Journal of Cleaner Production* 29-30: 208-213

Beerstecher E. (1954) Petroleum Microbiology. *Elsevier*

Cavicchioli, R., (2002) Extremophiles and the search for extraterrestrial life. *Astrobiology* 2:281-292

Cervantes, C., G. Ji, J.L. Ramírez, S. Silver (1994) Resistance to arsenic compounds in microorganisms. *FEMS Microbiology Reviews* 15: 355-367

Costagliola P., M. Benvenuti, L. Chiarantini, S. Bianchi, F. Di Benedetto, M. Paolieri, L. Rossato (2008) Impact of ancient metal smelting on arsenic pollution in the Pecora River Valley, Southern Tuscany, Italy. *Applied Geochemistry* 23(5): 1241-1259

Costagliola P., M.M. Benvenuti, M.G. Benvenuti, F. Di Benedetto, P. Lattanzi (2010) Quaternary sediment geochemistry as a proxy for toxic element source: A case study of arsenic in the Pecora Valley (southern Tuscany, Italy) *Chemical Geology* 270(1-4): 80-89

Dhami N.K., M.S. Reddy, A. Mukherjee (2013) Biomineralization of calcium carbonates and their engineered applications: a review. *Frontiers in Microbiology* 4: 1-13

Di Benedetto F. et al., (2011) Biotic and inorganic control on travertine deposition at Bullicame 3 spring (Viterbo, Italy): A multidisciplinary approach. Geochimica et Cosmochimica Acta 75: 4441-4455

Dixit S., J.G. Hering (2003) Comparison of Arsenic(V) and Arsenic(III) Sorption onto Iron Oxide Minerals: Implications for Arsenic Mobility *Environmental Science & Technology* 37: 4182-4189

Ehrlich H.L. & Newman D.K. (2008) Geomicrobiology, Fifth Edition *CRC Press, Taylor & Francis Group*

Hazen R.M., D. Papineau, W. Bleeker, R.T. Downs, J.M. Ferry, T.J. McCoy, D.A. Sverjensky, H. Yang (2008) Mineral evolution. *American Mineralogist*,93: 1693-1720

Kohnhauser K. (2007) Introduction to Geomicrobiology *Blackwell Science Ltd*

Kuznetsov S.I., Ivanov M.V., Lyalikova N.N. (1963) Introduction to Geological Microbiology (English Translation) *McGraw-Hill*

Lewin J. (1965) Calcification. In: Lewin R.A. (1965) Physiology and Biochemistry of Algae. *New York Academic Press*, pp. 457–465.

Luther S., N. Borgfeld, J. Kim, J.G. Parsons (2012) Removal of arsenic from aqueous solution: A study of the effects of pH and interfering ions using iron oxide nanomaterials *Microchemical Journal* 101: 30-36

Malasarn, D., C.W. Saltikov, K.J.M. Campbell, J.M. Santini, J.G. Hering, D.K. Newman (2004) *arr*A is a reliable marker for As(V) respiration. *Science* 306: 455

Nadson G.A. 1928. Beitrag zur Kenntniss der bakteriogenen Kalkablagerung. *Archiv für Hydrobiologie* 191:154-164.

Nicholson W.L., N. Munakata, G. Horneck, H.J. Melosh, P. Setlow 2000. Resistance of *Bacillus* endospores to extreme terrestrial and extraterrestrial environments. *Microbiological Molecular Biology Reviews* 64:548-572

Oremland R.S. and J.F. Stolz (2003) The Ecology of Arsenic. Science Vol. 300: 939-944

Pentecost A. (1988) Growth and calcification of the cyanobacterium *Homeothrix crustacea*. *Journal of General Microbiology* 134:2665-2671

Russell M.J, Ingham J.K., Zedef V., Maktav D., Sunar F., Hall A.J., Fallick A.E. (1999) Search for signs of ancient life on Mars: expectations from hydromagnesite microbialites, Salda Lake, Turkey. *Journal of the Geological Society*, 156:869-888

Silver S. and Phung L.T. (2005) Genes and Enzymes Involved in Bacterial Oxidation and Reduction of Inorganic Arsenic. *Applied and Environmental Microbiology* 71(2): 599-608

Smedley P.L., D.G. Kinniburgh, (2002) A review of the source, behaviour and distribution of arsenic in natural waters, *Applied Geochemistry* 217: 517-568.

Stumm W. & Morgan J.J. (1981) Aquatic Chemistry. An Introduction Emphasizing Chemical Equilibria in Natural Waters. *Wiley*

Warren L.A., P.A. Maurice, N. Parmar, F. Ferris (2001) Microbially mediated Calcium Carbonate precipitation: Implications for interpreting calcite precipitation and for solid-phase capture of inorganic contaminants. *Geomicrobiology Journal* 18(1): 93-115

Yoshida T, Yamauchi H, Sun GF (2004) Chronic health effects in people exposed to arsenic via the drinking water: dose-response relationships in review. *Toxic Applied Pharmacology* 198:243-252